Characterization of Particulate Matter Emissions from On-Road Gasoline and Diesel Vehicles Using a Soot Particle Aerosol Mass Spectrometer

Timothy R. Dallmann[1,a], Timothy B. Onasch[2], Thomas W. Kirchstetter[1,3], David R. Worton[4,5], Edward C. Fortner[2], Scott C. Herndon[2], Ezra C. Wood[6], Jonathan P. Franklin[2,b], Douglas R. Worsnop[2], Allen H. Goldstein[1,4], and Robert A. Harley[1,*]

[1]Department of Civil and Environmental Engineering
University of California, Berkeley, CA 94720-1710

[2]Aerodyne Research, Inc., Billerica, MA 01821

[3]Environmental Energy Technologies Division
Lawrence Berkeley National Laboratory, Berkeley, CA 94720

[4]Department of Environmental Science, Policy and Management
University of California, Berkeley, CA 94720-1710

[5]Aerosol Dynamics, Inc.
Berkeley, CA 94710

[6]Department of Public Health
University of Massachusetts, Amherst, MA 01003-9303

[a]Current Address:
Center for Atmospheric Particle Studies
Carnegie Mellon University, Pittsburgh, PA 15213-3890

[b]Current Address:
Department of Civil and Environmental Engineering
Massachusetts Institute of Technology, Cambridge, MA 02139

*Corresponding author e-mail: harley@ce.berkeley.edu

ABSTRACT

Particulate matter (PM) emissions were measured in July 2010 from on-road motor vehicles driving through a highway tunnel in the San Francisco Bay area. A soot particle aerosol mass spectrometer (SP-AMS) was used to measure the chemical composition of PM emitted by gasoline and diesel vehicles at high time resolution. Organic aerosol (OA) and black carbon (BC) concentrations were measured during various time periods that had different levels of diesel influence, as well as directly in the exhaust plumes of individual heavy-duty (HD) diesel trucks. BC emission factor distributions for HD trucks were more skewed than OA distributions (N=293), with the highest 10% of trucks accounting for 56 and 42% of total measured BC and OA emissions, respectively. OA mass spectra measured for HD truck exhaust plumes show cycloalkanes are predominate in exhaust OA emissions relative to saturated alkanes (i.e., normal and iso-paraffins), suggesting that lubricating oil rather than fuel is the dominant source of primary organic aerosol (POA) emissions in diesel vehicle exhaust. This finding is supported by the detection of trace elements such as zinc and phosphorus in the exhaust plumes of individual trucks. Trace elements were emitted relative to total OA at levels that are consistent with typical weight fractions of commonly used additives present in lubricating oil. A comparison of measured OA and BC mass spectra across various sampling periods revealed a high degree of similarity in OA and BC emitted by gasoline and diesel engines. This finding indicates a large fraction of OA in gasoline exhaust is lubricant-derived as well. The similarity in OA and BC mass spectra for gasoline and diesel engine exhaust is likely to confound ambient source apportionment efforts to determine contributions to air pollution from these two important sources.

1. INTRODUCTION

On-road motor vehicles, especially diesel engines, are important sources of fine particulate matter ($PM_{2.5}$) emissions (Dallmann et al., 2010). Exposure to $PM_{2.5}$ has been linked to various negative health effects (Pope and Dockery, 2006; Brook et al., 2010). $PM_{2.5}$ emissions from motor vehicles are of particular importance in urban areas where emissions occur in close proximity to exposed populations (Jerrett et al., 2005; Brugge et al., 2007). For example, the fraction of primary emissions that is inhaled by people is approximately an order of magnitude greater for vehicles operating in urban areas compared to coal-fired power plants that have tall stacks and tend to be in more remote locations (Evans et al., 2002; Marshall et al., 2005). Motor vehicle exhaust $PM_{2.5}$ is primarily composed of carbonaceous species, including black carbon (BC) and organic aerosol (OA). The relative abundance of BC depends on various factors, including engine type, engine operating conditions, and the presence of emission control equipment (Chow et al., 2011). In general, diesel engines tend to have higher BC emission rates relative to OA, and conversely for gasoline engines (Ban-Weiss et al., 2008; Chow et al., 2011).

Exhaust OA emissions consist of low volatility organic compounds derived from fuel and lubricating oil. Recent studies of emissions from combustion sources have shown that exhaust OA is semi-volatile, and undergoes gas-particle phase partitioning (Robinson et al., 2007; Grieshop et al., 2009). Partitioning of semi-volatile organic compounds (SVOC) between the condensed and gas phases is thought to be governed by absorptive partitioning in the atmosphere (Pankow, 1994) and therefore depends on temperature, concentrations of the condensed organic phase, and the SVOC volatility distribution (Donahue et al., 2006; Robinson et al., 2010). In the case of motor vehicle emissions, where BC/OA ratios are typically higher than observed in the

93 atmosphere, sorption of organic compounds to BC particle surfaces may also influence gas-
94 particle partitioning (Roth et al., 2005). Upon emission, rapid cooling of motor vehicle exhaust
95 promotes condensation of organic vapors and partitioning is shifted towards the particle phase.
96 As exhaust is diluted with ambient air, concentrations of gaseous SVOC are reduced, leading to
97 evaporation of SVOC to maintain phase equilibrium (Robinson et al., 2010). Measurements of
98 OA emission factors for motor vehicles are thus dependent on dilution and temperature
99 conditions of the sampled exhaust (Lipsky and Robinson, 2006; Grieshop et al., 2009).
100
101 The relative contributions of diesel fuel and lubricating oil to OA emissions depend on fuel and
102 lubricating oil properties, temperature, engine operating speed, engine load, and engine age and
103 condition (Kweon et al., 2003; Lapuerta et al., 2003; Sakurai et al., 2003; Brandenberger et al.,
104 2005; Maricq, 2007). Several laboratory and on-road investigations of diesel exhaust using
105 aerosol mass spectrometers and similar instruments have concluded that lubricating oil is the
106 dominant source of exhaust OA, based on comparisons of OA mass spectra for diesel exhaust,
107 diesel fuel, and lubricating oil (Tobias et al., 2001; Sakurai et al., 2003; Canagaratna et al., 2004,
108 Worton et al., 2014). Other researchers employing apportionment methods utilizing molecular
109 markers to distinguish between fuel and lubricant-derived OA report larger contributions from
110 fuel (Kleeman et al., 2008; Sonntag et al., 2012). The divergent findings reported in the literature
111 on the nature and sources of primary organic aerosol emissions in motor vehicle exhaust are not
112 easily reconciled.
113
114 Minor components of motor vehicle exhaust PM include inorganic species such as sulfate and
115 other trace elements (Kittelson et al., 2006; Maricq, 2007). Sulfur is present as an impurity in

fuel and is also used in additives found in lubricating oil. Trace elements, including zinc, phosphorus, calcium, and magnesium are commonly used in lubricating oil additives (Cadle, 1997; Spikes, 2004; Maricq, 2007). Emission rates of these trace elements in exhaust PM are low relative to carbonaceous species. However, trace metals may enhance the toxicity of particles emitted by motor vehicles (Gerlofs-Nijland et al., 2007; Bell et al., 2009). Also, for diesel engines, emissions of lubricant-derived elements are the focus of increasing scrutiny due to their potential negative effects on the performance of advanced emission control systems such as diesel particle filters. Lubricant-derived trace elements are not effectively removed during normal filter regeneration processes and thus have a tendency to form incombustible ash deposits on particle filters, which may degrade the performance and durability of these new control technologies (Sappok and Wong, 2011; Cross et al., 2012).

The primary objective of this study is to characterize the chemical composition of motor vehicle exhaust particulate matter emissions using a soot particle aerosol mass spectrometer. Individual chemical components of the exhaust PM emitted by large numbers of in-use gasoline and diesel-powered vehicles were measured to determine the composition of vehicular PM emissions, and to investigate the origins of OA emitted in diesel exhaust. This study also presents novel measurements made at high time resolution of lubricant-derived trace elements in the exhaust plumes of individual diesel trucks.

2. METHODS

2.1 Field Measurement Site

Motor vehicle emissions were measured in July 2010 at the Caldecott tunnel in Oakland, CA. These measurements were made as a part of a study that also quantified gas and particle phase pollutant emission factors for heavy-duty (HD) diesel trucks (Dallmann et al., 2012) and light-duty (LD) gasoline vehicles (Dallmann et al., 2013). All measurements of the exhaust particle emissions described here were made in bore 1 of the tunnel, which carries a mix of gasoline-powered passenger vehicles as well as medium-duty (MD) and HD diesel trucks. MD trucks are defined in this study as those with two axles and six tires (i.e., four tires on the rear axle). HD trucks are defined as those having three or more axles. Further information on the vehicle classification system used here can be found in Dallmann et al. (2013). The tunnel is 1 km long and bore 1 contains two lanes of eastbound traffic, with vehicles driving uphill on a 4% roadway grade. Sampling was conducted on four weekdays (July 22, 23, 26, 27) and two weekend days (July 24, 25), with analytical instrumentation operating from 10 AM – 6 PM each day.

As described in Dallmann et al. (2012), measurements of individual diesel exhaust plumes were made throughout the day on each of the four weekdays. In addition, 2-hr intensive operating periods (IOPs) were specified for each day of sampling, during which vehicles were counted and classified, and filter samples of particulate matter were collected. Sampling dates and times were chosen to study the impact of varying levels of diesel truck traffic on tunnel pollutant concentrations and emission factors. Two IOPs were conducted on each weekday, from 12-2 PM and 4-6 PM. On the weekend, there was only one IOP per day, from 2-4 PM. The midday (12-2 PM) IOPs on weekdays corresponded to the highest levels of diesel truck traffic in bore 1,

measured both by absolute numbers of trucks and as a fraction of total vehicle counts. LD vehicle activity was highest during the weekday late afternoon (4-6 PM) IOPs, which led to a relatively low diesel truck fraction during these times. While LD vehicle traffic volumes during the weekend IOPs were similar to weekday levels, diesel truck traffic activity was much lower on the weekend.

2.2 Measurement Methods

A new soot particle aerosol mass spectrometer (SP-AMS) described by Onasch et al. (2012) was used in this study to measure PM mass concentrations and chemical composition. The SP-AMS adds a 1064 nm continuous wave intra-cavity laser vaporizer to an existing Aerodyne high resolution aerosol mass spectrometer (HR-AMS). In the standard HR-AMS configuration, sampled particles are focused into a narrow beam using an aerodynamic lens. This particle beam is transmitted through a vacuum system to a resistively heated tungsten vaporizer at 600°C, on which particles impact and vaporize. Neutral molecules formed by the vaporization of non-refractory particle components (e.g. organic compounds, ammonium, sulfate, nitrate) are subsequently ionized by 70 eV electron impact ionization and detected by high resolution time-of-flight mass spectrometry (Jayne et al., 2000; DeCarlo et al., 2006). In the standard HR-AMS, lower volatility refractory materials such as black carbon (BC) are not vaporized at the operating temperatures of the tungsten vaporizer and, thus, are not detected by the instrument.

The inclusion of a laser vaporization source in the SP-AMS enables the characterization of refractory particles in addition to the standard components (e.g., organics, sulfate, nitrate, ammonium). The laser cavity is incorporated into the AMS vacuum chamber perpendicular to

182 the incident particle beam. As particles cross the laser beam, absorbing BC particles heat up to
183 several thousand degrees Kelvin before vaporizing into neutral carbon clusters (Onasch et al.,
184 2012). As the BC component of sampled particles is heated by IR absorption, both BC and any
185 coatings associated with these particles are vaporized and detected. Coating species may include
186 organics, inorganics, and refractory metals. Transit times for particles passing through the laser
187 beam are on the order of 5-20 μs. Due to the high vacuum in the ionizer chamber and short time
188 scales for vaporization, the likelihood of significant oxidation of particulate material is low.
189 Particles that either do not intersect with the laser beam or that pass through the laser beam
190 without vaporizing will impact on the tungsten vaporizer, where non-refractory components are
191 vaporized. Ionization and detection of vapor molecules in the SP-AMS follows standard HR-
192 AMS methods.
193
194 For the measurements presented here, both the tungsten and laser vaporizer of the SP-AMS were
195 turned on, enabling the characterization of non-refractory PM species and refractory BC along
196 with associated coatings. A focus of this project was to characterize the chemical composition of
197 particles in individual diesel truck exhaust plumes. These truck plume events occur over short
198 (typically < 30 s) time intervals and thus, fast sampling modes for the SP-AMS were prioritized.
199 In general, the SP-AMS was operated in the mass spectrum (MS) data acquisition mode,
200 whereby the particle beam is alternatively transmitted and blocked using a chopper wheel. Mass
201 spectra measured while the particle beam is blocked correspond to the instrument background
202 and are subtracted from the mass spectra measured while the particle beam is transmitted to
203 isolate the signal for each ensemble of sampled particles (DeCarlo et al., 2006; Kimmel et al.,
204 2011). This operating mode enabled the characterization of particle mass spectra with a nominal

time resolution of 1 s. Instrument background measurements (i.e. particle beam blocked) were conducted for 20 seconds of every 120 second sampling cycle. The time-of-flight mass spectrometer was operated with ion optics in the V-mode setting, which provided a mass resolving power of 2500 at 200 amu. This resolution enabled the separation of individual chemical ions at the same nominal mass-to-charge (m/z) ratio in particle mass spectra.

The SP-AMS was set up in the Aerodyne mobile laboratory, which was parked at the east end of the tunnel. As described in Dallmann et al. (2012), additional instruments to characterize gas and particle-phase pollutants were set up in the mobile lab and in a ventilation duct directly above the tunnel traffic. Tunnel air samples were drawn from a position approximately 0.1 m below the ceiling of the traffic bore through a ventilation plenum on the floor of the ventilation duct approximately 50 m from the tunnel exit. Air samples were delivered continuously to instruments set up in the mobile lab through 35 m of 1.4 cm inner diameter copper tubing at a flow rate of 16.7 l min^{-1}. A URG (Chapel Hill, NC) cyclone was installed upstream of the aerosol instrumentation to remove particles with aerodynamic diameters larger than 2.5 μm.

Use of the long sampling line to deliver tunnel air samples to instruments located in the mobile lab led to significant diffusive losses of small particles. The particle transmission efficiency as a function of particle diameter for the extractive sampling technique used here was quantified using a combination of experimental measurements and theoretical calculations. A more detailed description of these methods is included in the Supplemental Information. Results indicated that there was 50% particle transmission through the sampling line for 50 nm diameter particles. Smaller (i.e., nuclei mode) particles were not efficiently transported through the sampling line.

Sampling losses of larger particles (>100 nm in diameter) are estimated to be less than 10%. Previous measurements of particle size distributions at the Caldecott tunnel show that while sub-50 nm particles account for the majority (>75%) of total particle number emissions in motor vehicle exhaust, the contribution of these ultrafine particles to total particle volume and mass is relatively minor (<10%) (Ban-Weiss et al., 2010). Thus, while the long sampling line used here is not well suited for describing total particle number concentrations or ultrafine particle size distributions, characterization of particle mass concentrations and chemical composition is not expected to be significantly impacted by sampling line losses.

Additional instrumentation deployed at the Caldecott tunnel provided supporting data for the interpretation and analysis of the SP-AMS data. A full description of gas and particle phase species measured at the tunnel and corresponding instrumentation is presented in companion publications (Dallmann et al., 2012; 2013). Supporting data utilized in this study include non-dispersive infrared absorption measurements of CO_2 concentration (LI-COR model LI-6262, Lincoln, NE), and BC mass concentrations measured with a multi-angle absorption photometer (MAAP, ThermoFisher Scientific model 5012, Waltham, MA). Additionally, average mass concentrations of OA, BC, and $PM_{2.5}$ were quantified for each 2-hr sampling period using thermal-optical and gravimetric analyses of collected quartz and Teflon filter samples, respectively.

2.3 Data Analysis

The SP-AMS data were processed using standard HR-AMS software toolkits SQUIRREL (Sequential Igor Data Retrieval, version 1.52C) and PIKA (Peak Integration by Key Analysis,

version 1.11C). The direct measurement provided by the SP-AMS is a summed ion rate for individual chemical species (I_s, units of Hz = ions s^{-1}). This ion rate can be converted into a mass concentration (C_s, μg m^{-3}) utilizing instrument calibrations and known sample flow rate (Q = 1.4 cm^3 s^{-1}) (Jimenez et al., 2003; Allan et al., 2004; Onasch et al., 2012):

$$C_s = \frac{\sum_i I_{s,i}}{CE_s \times RIE_s \times mIE_{NO_3} \times Q} \quad (1)$$

where mIE_{NO3} is the mass specific ionization efficiency for nitrate (ions measured per picogram of nitrate sampled), CE_s is the SP-AMS collection efficiency for species S, and RIE_s is the relative ionization efficiency of species S, and is defined as the ratio of the mass specific ionization efficiency of particulate species S to mIE_{NO3}. mIE_{NO3} was determined to be 600 ± 120 ions $picogram^{-1}$ based on standard AMS ammonium nitrate instrument calibrations performed during the field sampling campaign. RIE_s values for nonrefractory species typically measured by HR-AMS instruments have been characterized through laboratory calibrations (Alfarra et al., 2004; Canagaratna et al., 2007). Similarly, RIE_{BC} was experimentally determined to be 0.2 ± 0.1 based on laboratory calibrations using aerosolized Regal black particles (Onasch et al., 2012).

The laser vaporization source utilized in the SP-AMS extends the range of chemical species detected by the instrument to include refractory species associated with BC containing particles, such as metals derived from lubricating oil additives. Experimentally derived RIE_s values are not available for these species. For ions generated by electron impact ionization, RIE_s values can be estimated from electron impact ionization cross-sections and number of electrons for the species of interest (Jimenez et al., 2003; Salcedo et al., 2012). Based on literature-reported electron

274 impact ionization cross-sections, RIE_s values for lubricant-derived trace species considered in
275 this study are estimated as 1 ± 0.3 (Pottie, 1966; Tawara and Kato, 1987; Freund et al., 1990;
276 Mozejko and Sanche, 2005). Calcium and magnesium ions may also be generated through
277 thermal ionization mechanisms, which would result in higher than expected ion signals for these
278 species and an overestimate of their sampled mass.
279
280 The collection efficiency in the denominator of Eq. 1 represents the fraction of sampled particles
281 that are detected by the SP-AMS and is dependent on the chemical and physical properties of
282 sampled particles and their interactions with the laser and tungsten vaporizers (Matthew et al.,
283 2008). The CE for non-refractory species, which can be vaporized by both the laser and tungsten
284 vaporizers, is governed by losses due to particle bounce effects at the tungsten vaporizer, and is
285 assumed to be equal to 1 (i.e., negligible losses) for the motor vehicle exhaust emissions
286 considered here (Slowik et al., 2004; Matthew et al., 2008; Onasch et al., 2012). The CE value
287 for refractive BC is largely dependent on the degree of overlap in the particle and laser beams,
288 and was estimated through comparison with a collocated MAAP instrument, as discussed below.
289 SP-AMS collection efficiencies for lubricant-derived trace species have not yet been empirically
290 characterized. CE values will depend on the interactions of these species with the laser and
291 tungsten vaporizers. Species with boiling points below the operating temperature of the tungsten
292 vaporizer (e.g. phosphoric acid, boiling (decomposition) point = 158 ºC) are likely readily
293 vaporized at both vaporizers and have similar CE values to non-refractory species. Species with
294 boiling points above the operating temperature of the tungsten vaporizer may still generate ion
295 signals from both vaporizers and thus have CE values between refractory BC (laser only) and
296 non-refractory species. Salcedo et al. (2012) demonstrated the capability of a tungsten vaporizer

operated at 600 ºC to vaporize zinc (boiling point = 907 ºC) in ambient air samples, though time scales for evaporation were slower than for non-refractory species. More refractory species such as calcium and magnesium (boiling point = 1484 and 1090 ºC, respectively) are likely vaporized more readily through the heating of BC particles at the laser vaporizer. Based on these considerations, CE values for the lubricant-derived trace species are estimated as unity with the same uncertainty as non-refractory species (20%) for phosphorus/phosphate and with greater uncertainty (50%) for zinc. Due to the higher level of uncertainty in the vaporization and ionization mechanisms for calcium and magnesium, ion signals were not converted to mass concentrations for these species.

2.4 Diesel Truck Exhaust Plume Analysis

The fast time response SP-AMS operating mode used for this project enabled the characterization of average mass spectra and chemical species emission factors for individual diesel truck exhaust plumes. Video recordings of vehicle activity at the tunnel on each day of sampling (weekdays only; 10 AM-6 PM) were analyzed to determine the times at which individual HD trucks passed beneath air sampling inlets. Instances where an individual truck passage resulted in a rise and fall (peak) in the measured CO_2 concentration discernible above background tunnel levels were identified in previous work (Dallmann et al., 2012), and are used as the basis for further data analysis including SP-AMS results presented here. Observed CO_2 concentration peaks were used to delineate the time period of exhaust plume capture for each passing truck. Corresponding peaks in measured concentrations of other pollutants are indicative of their presence in the exhaust plume, and provide information on the emission profile of each truck. In this study, mass spectra for individual trucks were obtained by subtracting the tunnel

320 background mass spectrum measured immediately prior to sampling of a truck plume from the
321 average mass spectrum measured during the truck plume event. Fuel-based emission factors for
322 particulate species were calculated following the carbon balance method (Dallmann et al., 2011;
323 2012):
324

325 $$EF_S = \frac{\int_{t_1}^{t_2}([S]_t - [S]_{t_1})dt}{\int_{t_1}^{t_2}([CO_2]_t - [CO_2]_{t_1})dt} w_c \quad (2)$$

326

327 where EF_S is the emission factor for particulate species S (g kg fuel^{-1}) and $w_c = 0.87$ is the weight
328 fraction of carbon in diesel fuel. The period of exhaust plume measurement is represented by the
329 time interval $t_1 \leq t \leq t_2$. $([S]_t - [S]_{t1})$ is the tunnel background-subtracted concentration of species
330 S at time t (μg m^{-3}), and similarly for $[CO_2]$ (mg C m^{-3}). Carbon dioxide concentrations are
331 typically much larger than those of other carbon-containing species in diesel exhaust and thus,
332 CO_2 is used here to estimate total fuel-derived carbon associated with the exhaust plume.
333

334 **3. RESULTS AND DISCUSSION**

335 ***3.1 Instrument Intercomparisons and IOP Average Concentrations***

336 The ability of the SP-AMS to measure BC emitted by motor vehicles was evaluated through a
337 comparison with a collocated MAAP absorption photometer. Black carbon concentrations
338 measured with the MAAP were in good agreement with other approaches (e.g. aethalometer,
339 photoacoustic spectrometer, thermal-optical analysis of quartz filters) used to characterize BC
340 during this field campaign (Dallmann et al., 2012). Figure 1 shows a comparison of 10 s average
341 BC concentrations measured by SP-AMS and MAAP for four of the six days of sampling

342 considered here. This comparison does not include July 23 or 24, as the MAAP was offline on
343 those days. In general, BC concentrations measured by the two instruments are well correlated,
344 with $R^2 = 0.92$ based on a linear least squares fit of the data. On average, MAAP BC
345 concentrations are approximately four times larger than SP-AMS BC concentrations. In a
346 previous application of the SP-AMS to measure particulate matter emitted by motor vehicles,
347 Massoli et al. (2012) report a factor of nine underestimate in BC concentrations measured by SP-
348 AMS relative to the MAAP. The authors attribute this disparity to particle losses within the SP-
349 AMS resulting from sub-optimal alignment of the laser vaporizer and particle beams. In cases
350 where regions of the particle beam do not overlap with the laser beam, BC particles are not
351 vaporized and thus are not detected (Onasch et al., 2012). The slope of the linear fit to the data
352 shown in Figure 1 therefore defines the effective collection efficiency of the SP-AMS with
353 respect to the BC component of sampled PM, CE = 0.27. Based on this analysis, SP-AMS BC
354 mass concentrations presented here are multiplied by a factor of 3.7 (i.e., 1/CE).
355

356 SP-AMS measurements of carbonaceous aerosol mass concentrations for each IOP are shown in
357 Figure 2, together with corresponding measurements of BC and OA derived from thermal-optical
358 analysis of quartz filter samples, and $PM_{2.5}$ mass concentrations from gravimetric analysis of
359 Teflon filter samples. In this figure, tunnel $PM_{2.5}$, OA, and BC mass concentrations are shown in
360 blue, green and black, respectively. For quartz filter OA measurements presented in Figure 2,
361 quartz filters located behind (i.e., downstream of) teflon filters (QBT) were used to correct for a
362 positive sampling artifact in determining tunnel OA concentrations from front quartz filters. The
363 positive artifact results from the adsorption of low volatility organic vapors to the quartz filters.
364 Volatilization of collected OA from the front quartz filter may result in a negative sampling

365 artifact, though this effect has been found to be small relative to the adsorption of organic vapors
366 for emissions from gasoline and diesel engines (Schauer et al., 2002; Shah et al., 2004; Lipsky
367 and Robinson, 2006; May et al., 2013). Tunnel OA concentrations were estimated by subtracting
368 organic mass measured on QBT filters from bare quartz filters collected in parallel. Resulting
369 OA concentrations for each IOP are shown in Figure 2 as solid green bars (Q-QBT). The
370 measured organic concentration derived from QBT filter samples (corresponding to adsorbed
371 organic vapors) is shown as unshaded bars above the corrected front quartz filter OA estimates.
372 Organic carbon mass loadings determined from the quartz filters were converted to equivalent
373 OA mass by multiplying by a factor of 1.25. This factor represents the organic aerosol to organic
374 carbon mass ratio (OA/OC) and accounts for additional mass, mainly hydrogen, associated with
375 organic carbon present in the particle phase. The OA/OC ratio for PM in the Caldecott tunnel
376 was calculated using SP-AMS data following methods developed by Aiken et al. (2007, 2008).
377 Throughout the field study, SP-AMS OA concentrations were approximately 40% higher than
378 OA concentrations derived from the corrected quartz filter samples (Q-QBT). Uncertainties in
379 the quantification of these sampling artifacts likely contribute to the discrepancies observed in
380 filter and SP-AMS OA measurements. For example if the volatilization of particulate organic
381 compounds collected on front quartz filters is non-negligible, treatment of the back quartz filter
382 OA measurements followed here may underestimate actual tunnel OA concentrations.
383
384 As shown in Figure 2, fine particulate matter measured in the tunnel is composed primarily of
385 carbonaceous species. The sum of OA and BC contributions estimated from quartz filter samples
386 and the SP-AMS accounted for 87 ± 8 and 99 ± 8% of Teflon filter-derived $PM_{2.5}$ mass,
387 respectively. This finding is consistent with the knowledge that motor vehicle exhaust $PM_{2.5}$ is

388 mainly composed of carbonaceous species, with minor contributions from inorganic species such
389 as sulfate and metallic ash (Fujita et al., 2007; Maricq, 2007; Ban-Weiss et al., 2008). The largest
390 difference between $PM_{2.5}$ and carbonaceous aerosol mass concentrations was observed for the
391 July 22, 12-2 PM sampling period shown at the left of Figure 2. During this time period, tunnel
392 maintenance staff carried out street sweeping of the traffic lanes, which is expected to have
393 enhanced contributions to $PM_{2.5}$ from non-tailpipe sources (e.g., resuspended road dust).
394
395 Total $PM_{2.5}$ mass measurements provided by the SP-AMS, including carbonaceous species and
396 inorganic ions (e.g. sulfate, nitrate, ammonium, chloride), are further compared with Teflon filter
397 derived $PM_{2.5}$ mass concentrations in Figure 3. Excluding anomalous data from one sampling
398 period with street sweeping activity, $PM_{2.5}$ mass concentrations determined by the two methods
399 are generally in good agreement, with a slope near one and a correlation coefficient of 0.82.
400 Inorganic ions accounted for less than 5% of total particle mass measured by the SP-AMS during
401 weekday IOPs, and 8 and 14% of total mass on Saturday and Sunday sampling periods,
402 respectively, when tunnel concentrations were lower. Ammonium concentrations were well
403 correlated with the sum of the nitrate molar concentration and the sulfate molar concentration
404 multiplied by a factor of two (R^2=0.98), suggesting the main source of these species was likely
405 ammonium nitrate and ammonium sulfate present in the ambient background air drawn inside
406 the tunnel. Motor vehicle contributions to inorganic ions measured in the tunnel may also result
407 from the presence of trace impurities and additives in fuel and lubricating oil, particularly in the
408 case of sulfate (Maricq, 2007).
409
410

411 ***3.2 Chemical Composition of Diesel Exhaust PM***

412 The concentration time-series response of the SP-AMS to a passing HD truck is shown in Figure
413 4 for BC, OA, and several elements. A clear peak in the measured CO_2 concentration above
414 background levels is visible and defines the period of exhaust plume measurement (~15 s).
415 Corresponding peaks in the measured OA and BC concentrations are similarly well-defined,
416 indicating the presence of these species in the exhaust plume. Figure 4 also shows clear peaks in
417 several trace elements associated with diesel fuel and lubricating oil additives (Cross et al.,
418 2012).

419

420 A prior analysis of data collected during ~30 hours of sampling over the four weekdays
421 considered here identified 809 candidate HD trucks for which individual truck exhaust plume
422 contributions of CO_2 were discernible above background levels inside the tunnel (Dallmann et
423 al., 2012). Due to a lower duty cycle relative to CO_2 analyzers (i.e., frequent background
424 checking) and more frequent instrument calibrations, SP-AMS data were only available for 293
425 of the 809 successful plume captures. As discussed below, this sub-sample was used to calculate
426 emission factors for OA, BC, and various trace elements from individual trucks. For the mass
427 spectral analysis discussed here, additional criteria were defined to identify trucks for which
428 exhaust plume PM mass spectra were sufficiently distinct from tunnel background mass spectra.
429 In this case, only trucks with OA and BC emission factors greater than 0.05 g kg^{-1}, as calculated
430 using Eq. 2, and peak exhaust plume CO_2 concentrations at minimum 100 ppm higher than
431 tunnel background levels (corresponding to an ~10% increase for typical tunnel CO_2
432 concentrations of 1000 ppm) were considered for mass spectral analysis. These criteria excluded
433 trucks with low particle mass emission rates and truck plumes that were highly dispersed in the

434 tunnel prior to their measurement. Of the 293 trucks for which SP-AMS data were available, 145
435 met these acceptance criteria.

436

437 The average SP-AMS mass spectrum for this population of trucks is shown in Figure 5, with
438 mass spectra for carbon and organic ions shown in the lower panel and ions associated with trace
439 elements shown in the top panel. Tunnel background-subtracted mass spectra for each truck were
440 normalized to the total ion signal and then averaged to obtain the results shown in Figure 5. In
441 the average diesel PM mass spectrum, the height of each bar indicates the relative percent of the
442 total ion signal for a given mass-to-charge ratio (m/z), and uncertainty bars show the 95%
443 confidence interval. The use of a high-resolution mass spectrometer enabled identification of
444 individual chemical ion contributions at the same nominal m/z and the separation of spectra
445 according to chemical families. Ion fragments of the family C_x^+ indicate clusters of carbon atoms
446 and represent the BC signal, shown in black in Figure 5. On average, the BC signal accounted for
447 approximately 9% of the total ion signal measured for diesel exhaust PM. The largest carbon ion
448 signals are from the fragments C_1^+ (m/z=12) and C_3^+ (m/z=36), which together account for 77%
449 of the total carbon ion signal for m/z in the range 10-360. Likewise, small carbon clusters of 1-5
450 carbon atoms (C_1^+-C_5^+) account for greater than 97% of the total carbon ion signal in this mass
451 range. These findings are consistent with previous measurements of BC mass spectra for
452 individual diesel buses in New York City (Massoli et al., 2012).

453

454 The OA component of the diesel truck mass spectrum is dominated by hydrocarbon ion
455 fragments of the $C_xH_y^+$ family. The largest observed signals in the OA mass spectrum are from

456 the ion fragments $C_3H_5^+$ (m/z = 41), $C_3H_7^+$ (m/z = 43), $C_4H_7^+$ (m/z = 55), and $C_4H_9^+$ (m/z = 57),
457 which together account for 27 and 30% of the total ion and OA ion signals, respectively. In sum,
458 ions of the $C_xH_y^+$ family contributed 91% of the measured OA signal and 79% of the total ion
459 signal. The predominance of the $C_xH_y^+$ family in the OA mass spectrum is expected for primary
460 exhaust OA from diesel engines and is consistent with previous characterizations of the chemical
461 composition of PM emitted by in-use vehicles (Canagaratna et al., 2004; Chirico et al., 2011;
462 Massoli et al., 2012). Organic aerosol emitted by diesel trucks is largely unoxidized, with
463 oxidized organic ion fragments of the families CHO and $CHO_{>1}$ contributing less than 10% of
464 the total organic signal. Atomic ratios (O/C, H/C) and the organic aerosol mass to organic carbon
465 ratio (OA/OC) of the diesel truck OA were evaluated following methods developed by Aiken et
466 al. (2007, 2008). Average values of O/C, H/C, and OA/OC for the diesel trucks considered here
467 are 0.06 ± 0.02, 1.90 ± 0.05, and 1.24 ± 0.03, respectively. These values agree with other ratios
468 measured in laboratory investigations of diesel engine exhaust (Mohr et al., 2009; Chirico et al.,
469 2010).
470
471 Sources of OA in diesel exhaust include unburned fuel and lubricating oil and their partially
472 oxidized products (Maricq, 2007). Though both fuel and oil are derived from petroleum sources,
473 different processing techniques lead to large differences in the molecular weights and chemical
474 structures. For example, diesel fuel is typically composed of hydrocarbons with carbon numbers
475 ranging from C_{10}-C_{25}, while lubricating oils consist of less volatile hydrocarbons with carbon
476 numbers ranging from C_{14}-C_{45} (Tobias et al., 2001; Kweon et al., 2003; Isaacman et al., 2012).
477 Additionally, while diesel fuels have high concentrations of n-alkanes, lubricating oils tend to be

478 dominated by cycloalkanes, due to the deliberate removal of n-alkanes during a dewaxing
479 process (Tobias et al., 2001; Isaacman et al., 2012).
480
481 Previous studies of diesel PM using AMS and similar instruments have investigated the relative
482 contributions of fuel and lubricating oil to diesel exhaust OA (Tobias et al., 2001; Sakurai et al.,
483 2003; Canagaratna et al., 2004). Three main hydrocarbon ion series were identified in both fuel
484 and lubricating oil: (1) $C_nH^+_{2n+1}$ (m/z 29, 43, 57, 71, 85, 99…) typical of saturated alkyl
485 compounds (n-alkanes, branched alkanes), (2) $C_nH^+_{2n-1}$ (m/z 27, 41, 55, 69, 83, 97…) typical of
486 unsaturated aliphatic compounds (cycloalkanes, alkenes) and (3) $C_nH^+_{2n-3}$ (m/z 67, 81, 95, 109…)
487 ion fragments derived from bicycloalkanes (McLafferty and Turecek, 1993; Tobias et al., 2001;
488 Canagaratna et al., 2004). Also, previous investigations found that saturated alkane ion signals
489 are larger than neighboring cycloalkane-derived ion signals in the ranges m/z = 67-71 and 81-85
490 for diesel fuel, while the opposite is true for lubricating oil (Tobias et al., 2001; Sakurai et al.,
491 2003; Canagaratna et al., 2004). In each of these prior studies, the predominance of m/z = 69
492 versus 71, and m/z = 83 versus 85, in diesel OA mass spectra indicates that the lubricating oil
493 contribution to diesel OA dominates over contributions attributable to diesel fuel.
494
495 All three of the main hydrocarbon series noted above are apparent in the diesel truck plume OA
496 mass spectrum measured in this study (shown in Figure 5). Average diesel PM ion signal ratios
497 at m/z = 69 to 71 and m/z = 83 to 85 were 1.51 ± 0.08 and 1.66 ± 0.08, respectively. Sakurai et
498 al. (2003) measured particle mass spectra for diesel exhaust particles and for mixtures of varying
499 ratios of lubricating oil to diesel fuel. Results from these experiments show ion signals at m/z 71
500 and 85 were larger than signals at m/z 69 and 83, respectively, for mixtures containing 20% fuel:

80% oil and 10% fuel: 90% oil. Cycloalkane signals in these mass ranges were only clearly dominant over saturated alkane signals for a mixture of 5% fuel: 95% oil. Based on these results, the authors concluded that measured diesel exhaust particles, whose spectra had ratios at m/z = 69 to 71, and m/z = 83 to 85 greater than unity, are comprised of at least 95% unburned lubricating oil. While the lack of measurements of pure fuel and lubricating oil samples preclude a similar analysis in the present study, ion ratios greater than one at m/z = 69 to 71 and m/z = 83 to 85 support a similar conclusion that lubricating oil was the predominant source of OA measured in the exhaust of diesel trucks operating in the Caldecott tunnel. Alkenes formed from incomplete combustion of diesel fuel may contribute to the signal measured at m/z = 69 and m/z = 83, though this contribution is expected to be minor relative to the cycloalkane signal (Worton et al., 2014).

Further information concerning the origin of OA in the exhaust of the 145 HD diesel trucks considered here is derived through an analysis of other trace elements measured in individual exhaust plumes. Trace elements included in this analysis were selected based on their inclusion in lubricating oil and on their prior identification in diesel exhaust PM in a laboratory study that used the SP-AMS (Cross et al., 2012). These trace species are typically present as additives or impurities in diesel fuel and lubricating oil. For example, zinc and phosphorus are present in zinc dialkyl dithiophosphate (ZDDP), a widely used lubricating oil additive that enhances antiwear and antioxidant properties of the oil (Spikes, 2004). Similarly, calcium and magnesium are components of detergent additives in lubricating oils (Cadle et al., 1997). Lubricating oil additives such as calcium, zinc, and phosphorus are typically not present at detectable levels in diesel fuel, and can thus be used as tracers for lubricant-derived OA in diesel exhaust (Spencer et

al., 2006; Shields et al., 2007). Sulfur is present both as a trace species in diesel fuel, as well as in lubricating oil additives. Other species considered here include potassium and sodium associated with diesel fuel, and lead associated with engine wear (Cross et al., 2012). While these trace elements typically account for a small fraction of the total PM mass emitted by diesel engines, trace element emissions may accumulate over time and negatively affect the performance of diesel particle filters, as ash deposits related to these species are not readily removed from exhaust filters by oxidative regeneration schemes that are used to remove accumulated BC and OA (Maricq, 2007; Sappok and Wong, 2011).

The top panel of Figure 5 shows the average relative ion signal measured for trace elements in the exhaust of diesel trucks operating at the Caldecott tunnel. The mass resolving power of the high resolution time-of-flight mass spectrometer used in the SP-AMS enabled the simultaneous identification of these trace elements and hydrocarbon fragments at the same nominal m/z. Included in the legend are the correlation coefficients for a comparison of the summed ion signal for each ion group with the total OA signal across the sampled population of trucks. For trace elements, the highest correlation with OA was observed for lubricant-derived species, including phosphorus containing ions (phosphorus/phosphate), zinc, and magnesium. Figure 4 shows an example of a truck plume where signals for these species were particularly strong and readily discernible above both background signals and SP-AMS instrument noise. Emission mechanisms for lubricating oil include volatilization of oil components at high temperatures and liquid oil emissions (Tornehed and Olofsson, 2011). In Figure 4, the correspondingly large BC signal suggests these elements were likely associated with BC particles and vaporized as a result of the heating of laser-light absorbing BC particles. Across the sampled truck population, the

identification of lubricant-derived species in exhaust PM is further supported by a positive correlation ($R^2 = 0.71$) between the average plume phosphorus/phosphate and zinc signals, suggesting a common source for both of these trace elements. The presence of lubricant-derived trace metal species in diesel exhaust plumes and their positive correlation with OA further suggests lubricating oil as a major contributor to diesel OA emissions.

In Figure 5, a clear signal for calcium, another common lubricating oil additive, is visible at m/z = 40, though the correlation with OA is weaker than for other lubricant-derived elements. Uncertainties arose in the definition of the exhaust plume calcium (^{40}Ca) signals due to interferences from the gas phase argon (Ar) signal at the same m/z. The mass resolving power of the SP-AMS was not sufficient to differentiate ^{40}Ca from ^{40}Ar. Argon levels in tunnel air are expected to be relatively stable, thus for this analysis signals for ^{40}Ca and ^{40}Ar were summed and any increase in the combined signal above baseline levels was assumed to represent a contribution from ^{40}Ca. Uncertainties due to the higher baseline signal in this approach may explain the larger diesel truck exhaust signal for calcium relative to other lubricant-derived species, as well as the weaker correlation with OA.

The average diesel truck BC mass spectrum, normalized to total carbon ion signal, is shown in Figure 6. A key feature of this spectrum is the low variability in the distribution of carbon ion signals across the sampled truck population, as evidenced by the relatively small uncertainty in contributions to the total signal associated with each carbon ion. This low variability suggests that the distribution shown in Figure 6 could define a BC emissions source “fingerprint” for in-

569 use diesel trucks that may be useful in future applications of the SP-AMS to source
570 apportionment of ambient BC (Onasch et al., 2012).
571
572 ***3.3 HD Diesel Truck Emission Factors***
573 Emission factors for individual chemical components of PM emitted by diesel trucks were
574 evaluated for the entire population of trucks for which SP-AMS data were available, including
575 low-emitting trucks not included in the mass spectral analysis presented above. Emission factors
576 were calculated using Eq. 2, and species considered here include OA, BC, zinc, and
577 phosphorus/phosphate. Fleet-average emission factors for a sample of 293 HD diesel trucks are
578 presented in Table 1, and emission factor distributions are shown in Figure 7. Note that trucks
579 with zero or negative emission factors calculated using Eq. 2 are not included in this figure. For
580 each of the emitted species considered here, between 5 and 11% of the total measurements were
581 for trucks with no detectable emissions. Both the OA and BC distributions are lognormal, though
582 the BC distribution is more skewed than OA: 10% of BC and OA measurements accounted for
583 56 and 42% of total emissions of the respective pollutants. The fleet-average BC emission factor
584 from the SP-AMS is 2.6 ± 0.8 times the value of the corresponding OA emission factor.
585 Resulting OA to BC (OA/BC) and OC to BC (OC/BC) mass emission ratios for diesel trucks are
586 0.38 ± 0.12 and 0.31 ± 0.10, respectively. A prior vehicle emission study at the Caldecott tunnel
587 estimated an OC/BC ratio for diesel trucks of 0.34, which is in good agreement with the ratio
588 reported here (Ban-Weiss et al., 2008). Because diesel PM is predominantly carbonaceous, the
589 sum of the OA and BC emission factors, 0.86 ± 0.17 g kg^{-1}, should provide a reasonable estimate
590 of the $PM_{2.5}$ emission factor for HD diesel trucks. Note that OA emission factors reported here
591 are representative of the dilution conditions of the individual exhaust plumes sampled. Further

592 dilution of exhaust to atmospheric levels may lead to volatilization of SVOC and a reduction in
593 primary OA mass (Lipsky and Robinson, 2006; Robinson et al., 2007). Dilution ratios for the
594 exhaust plume measurements reported here ranged from 60-3600, with an average (±95%
595 confidence interval) of 650 ± 60. HD truck BC and OA emission factors presented here are
596 approximately three times the values measured during a recent dynamometer test of an
597 uncontrolled HD diesel truck operating on an urban dynamometer driving cycle, though similar
598 OC/BC ratios were measured in both studies (May et al., 2014).
599
600 The ability of the SP-AMS to detect refractory PM components enabled the quantification of
601 lubricant-derived trace element emission factors for individual HD trucks. Fleet-average
602 emission factors for zinc and phosphorus/phosphate are reported in Table 1. Fleet-average
603 emission factors for lubricant-derived elements are on the order of 0.1-1 mg kg^{-1} and are nearly
604 three orders of magnitude lower than OA and BC emission factors. Emission factors reported
605 here agree to within a factor of 4 with emission factors derived from a near-roadway study at a
606 freeway in Los Angeles with high HD diesel truck activity (Ning et al., 2008). Emission factor
607 distributions for zinc and phosphorus/phosphate, shown in Figure 7, were lognormal and similar
608 to OA in their degree of skewness.
609
610 The ratio of each trace element emission factor to the fleet-average OA emission factor is
611 presented in Table 1, along with the weight fraction of each element in a CJ-4 diesel engine oil
612 as reported by Sappok and Wong (2011). Ratios define the emission factor for a given species to
613 the emission factor for OA, and reported units of ppm are equivalent to units of ppm used for
614 bulk lubricating oil weight fractions. In general, the measured emission factors for these

615 elements, when normalized to the OA emission factor, correspond well with their bulk oil
616 concentrations. For both zinc and phosphorus/phosphate, OA normalized emissions are within
617 25% of lubricant concentrations. Furthermore, the relative magnitudes of emission factors for
618 these trace species follow their abundances in lubricating oil. These findings further support the
619 conclusion that lubricating oil, rather than diesel fuel, was the dominant source of exhaust OA
620 emissions for trucks operating in the Caldecott tunnel. If a large fraction of OA emissions were
621 derived from unburned or partially oxidized fuel, emission factors for these trace elements would
622 be expected to be significantly lower when normalized to OA emissions.
623
624 ***3.4 Comparison of Diesel and Gasoline Exhaust PM***
625 Differences in PM emitted by gasoline and diesel motor vehicles were studied through a
626 comparison of the chemical composition of carbonaceous aerosols measured in the tunnel during
627 periods of varying diesel truck influence. Figure 8 shows the average BC and OA mass spectra
628 and relative mass concentrations for six different sampling periods/vehicle emission event types:
629 individual diesel exhaust plume measurements (sample of 145 trucks considered for mass
630 spectral analysis, top panel); four weekday 12-2 PM and 4-6 PM IOPs (second and third panels);
631 the Saturday and Sunday 2-4 PM IOPs (fourth and fifth panels); and a high PM-emitting gasoline
632 vehicle (bottom panel). The panels are thus arranged from top to bottom in order of decreasing
633 diesel engine influence. The relative contribution of diesel engines to vehicle-derived carbon for
634 each IOP was calculated using measured CO_2 concentrations and vehicle count data, and is
635 included in the label for each IOP in Figure 8. In general, PM contributions from individual
636 gasoline vehicles were not discernible above tunnel background levels, and the direct
637 characterization of PM composition for a representative sample of *individual* gasoline vehicle

638 exhaust plumes was not possible. In the case of the gasoline vehicle plume event shown in
639 Figure 8, a clear OA signal was associated with the passing of a small truck. Concurrent time-
640 resolved measurements of carbon monoxide, benzene, and toluene emissions support the
641 conclusion that this high-emitting vehicle was equipped with a gasoline engine.
642
643 A main feature of Figure 8 is the increasing trend in the OA to BC mass ratio with decreasing
644 diesel influence. On average, diesel trucks were found to emit 2.6 ± 0.8 times more BC than OA,
645 with a corresponding OA/BC ratio of 0.38 ± 0.12. For weekday 12-2 PM and 2-4 PM sampling
646 periods, when diesel trucks accounted for between 7 and 18% of total vehicle-derived carbon
647 dioxide emissions, concentrations of OA and BC were similar (OA/BC = 1.1). The OA/BC ratio
648 further increased to 2.3 during the Sunday afternoon sampling period, when diesel trucks
649 accounted for 2% of vehicle-derived carbon dioxide. For the high-emitting gasoline vehicle, PM
650 emissions consisted primarily of OA. Fleet-average OA and BC emission factors for light-duty
651 vehicles have been evaluated separately for this field campaign, and the corresponding OA/BC
652 emission ratio was 1.7 ± 0.6 (Dallmann et al., 2013). Thus, the increasing influence of gasoline
653 vehicles on the measured OA/BC ratio was observed in this study for weekend sampling periods
654 when the influence of diesel trucks was lower.
655
656 Though relative contributions of BC and OA varied significantly, there was very little difference
657 in the corresponding mass spectra among sampling periods, as shown in Figure 8. Here, the
658 diesel truck BC and OA mass spectra are selected as reference mass spectra. Black carbon mass
659 spectra shown in Figure 8 all have similar distributions of carbon ions, with the BC signal
660 dominated by C_1^+-C_3^+ carbon ions in each case. Black carbon mass spectra across all sampling

periods were highly correlated ($R^2 > 0.99$ in all cases) with the reference diesel truck spectrum shown in the top panel of Figure 8. Results from this study indicate that fuel-specific BC emission factors for diesel trucks are approximately 50 times greater than for LD gasoline vehicles (Dallmann et al., 2013). Consequently, diesel trucks contributed the majority of BC measured during the weekday 12-2 and 4-6 PM sampling periods, though HD trucks accounted for only 7-18% of vehicle-derived carbon dioxide. Thus, the high degree of correlation observed between the weekday IOPs and diesel truck BC mass spectra is expected. Even small numbers of diesel trucks observed in the tunnel during the Sunday IOP still may have contributed significantly to measured BC, though in this case light-duty vehicles are expected to be the dominant source of BC in the tunnel. The correspondence of the BC mass spectra for the Sunday sampling period and high-emitting gasoline vehicle with the diesel truck mass spectrum therefore suggests carbon ion distributions measured with the SP-AMS are similar for gasoline and diesel vehicle-derived BC. This in turn suggests that apportionment of gasoline versus diesel contributions to BC using SP-AMS carbon ion spectra may be difficult to achieve due to the similarity of the source profiles.

Similar to what was found for BC, varying levels of diesel truck traffic did not produce discernible differences in OA mass spectra measured with the SP-AMS. All OA spectra are dominated by ion fragments of the $C_xH_y^+$ family, with prominent peaks at m/z = 41, 43, 55, and 57. Organic aerosol mass spectra for the 2-hr weekday and weekend sampling periods and the high-emitting gasoline vehicle were all well-correlated ($R^2 > 0.98$) with the diesel truck OA mass spectrum.

Average O/C, H/C, and OA/OC ratios are reported in Table 2, and were generally in good agreement across sampling periods considered here. The OA/OC and O/C ratios were slightly higher during the Sunday IOP, possibly due to a higher relative contribution from more oxidized ambient PM during this sampling period. However, these differences were not significant and values are in line with prior characterizations of motor vehicle OA (Aiken et al., 2008). These results show, for the fleet of in-use vehicles measured at the Caldecott tunnel, OA emitted by gasoline and diesel vehicles produces similar mass spectra when characterized using the SP-AMS. As discussed previously, several lines of evidence indicate that lubricating oil was the dominant source of OA emitted by diesel trucks operating in the tunnel. Although there are differences in lubricating oil formulations used in gasoline and diesel engines, the chemical composition of the oils is similar, and distinct from both gasoline and diesel fuel (Rogge et al., 1993; Fujita et al., 2007). The similarity of OA mass spectra for gasoline vehicle-dominated sampling periods therefore suggests that a large fraction of OA emitted by gasoline vehicles is lubricant-derived as well. The high degree of similarity in the chemical composition of OA from both gasoline and diesel engines will again make it difficult to conduct ambient source apportionment studies to determine contributions to air pollution from these two important sources.

ACKNOWLEDGEMENTS

The authors thank Drew Gentner, Gabriel Isaacman, Berk Knighton, Steven DeMartini, and the Caltrans staff at the Caldecott tunnel for their assistance. This publication was made possible by EPA grant RD834553. Its contents are solely the responsibility of the grantee and do not necessarily represent the official views of the EPA. Further, EPA does not endorse purchase of commercial products or services mentioned herein.

REFERENCES

Aiken, A. C.; DeCarlo, P. F.; Jimenez, J. L. Elemental analysis of organic species with electron ionization high-resolution mass spectrometry. *Anal. Chem.* **2007**, *79*, 8350–8358.

Aiken, A. C.; DeCarlo, P. F.; Kroll, J. H.; Worsnop, D. R.; Huffman, J. A.; Docherty, K. S.; Ulbrich, I. M.; Mohr, C.; Kimmel, J. R.; Sueper, D.; Sun, Y.; Zhang, Q.; Trimborn, A.; Northway, M.; Ziemann, P. J.; Canagaratna, M. R.; Onasch, T. B.; Alfarra, M. R.; Prevot, A. S. H.; Dommen, J.; Duplissy, J.; Metzger, A.; Baltensperger, U.; Jimenez, J.L. O/C and OM/OC ratios of primary, secondary, and ambient organic aerosols with high-resolution time-of-flight aerosol mass spectrometry. *Environ. Sci. Technol.* **2008**, *42*, 4478-4485.

Alfarra, M. R.; Coe, H.; Allan, J. D.; Bower, K. N.; Boudries, H.; Canagaratna, M. R.; Jimenez, J. L.; Jayne, J. T.; Garforth, A. A.; Li, S.-M.; Worsnop, D. R. Characterization of urban and rural organic particulate in the Lower Fraser Valley using two Aerodyne Aerosol Mass Spectrometers. *Atmos. Environ.* **2004**, *38*, 5745–5758.

Allan, J. D.; Delia, A. E.; Coe, H.; Bower, K. N.; Alfarra, M. R.; Jimenez, J. L.; Middlebrook, A. M.; Drewnick, F.; Onasch, T. B.; Canagaratna, M. R.; Jayne, J. T.; Worsnop, D. R. A generalised method for the extraction of chemically resolved mass spectra from Aerodyne aerosol mass spectrometer data. *J. Aerosol Sci.* **2004**, *35*, 909–922.

Ban-Weiss, G. A.; McLaughlin, J. P.; Harley, R. A.; Lunden, M. M.; Kirchstetter, T. W.; Kean, A. J.; Strawa, A. W.; Stevenson, E. D.; Kendall, G. R. Long-term changes in emissions of nitrogen oxides and particulate matter from on-road gasoline and diesel vehicles. *Atmos. Environ.* **2008**, *42*, 220–232; DOI:10.1016/j.atmosenv.2007.09.049.

Ban-Weiss, G. A.; Lunden, M. M.; Kirchstetter, T. W.; Harley, R.A. Size-resolved particle number and volume emission factors for on-road gasoline and diesel motor vehicles. *Aerosol Sci.* **2010**, *41*, 5-12, DOI:10.1016/j.jaerosci.2009.08.001.

Bell, M. L.; Ebisu, K.; Peng, R. D.; Samet, J. M.; Dominici, F. Hospital admissions and chemical composition of fine particle air pollution. *Am. J. Respir. Crit. Care Med.* **2009**, *179*, 1115-1120, DOI: 10.1164/rccm.200808-1240OC.

Brandenberger, S.; Mohr, M.; Grob, K.; Neukom, H. P. Contribution of unburned lubricating oil and diesel fuel to particulate emission from passenger cars. *Atmos. Environ*. **2005**, *39*, 6985-6994, DOI:10.1016/j.atmosenv.2005.07.042.

764 Brook, R. D.; Rajagopalan, S.; Pope, C. A., III; Brook, J. R.; Bhatnagar, A.; Diez-Roux, A. V.;
765 Holguin, F.; Hong, Y.; Luepker, R. V.; Mittleman, M. A.; Peters, A.; Siscovick, D.; Smith, S.
766 C.; Whitsel, L.; Kaufman, J. D. Particulate matter air pollution and cardiovascular disease.
767 An update to the scientific statement from the American Heart Association. *Circulation* **2010**,
768 *121* (21), 2331–2378, DOI:10.1161/CIR.0b013e3181dbece1.

769 Brugge, D.; Durant, J. L.; Rioux, C. Near-highway pollutants in motor vehicle exhaust: a review
770 of epidemiologic evidence of cardiac and pulmonary health risks. *Environ. Health* **2007**, *6*
771 (23), DOI:10.1186/1476-069X-6-23.

772 Cadle, S. H.; Mulawa, P. A.; Ball, J.; Donase, C.; Weibel, A.; Sagebiel, J. C.; Knapp, K. T.;
773 Snow, R. Particulate emission rates from in-use high-emitting vehicles recruited in Orange
774 County, California. *Environ. Sci. Technol.* **1997**, *31*, 3405-3412.

775 Canagaratna, M. R.; Jayne, J. T.; Ghertner, D. A.; Herndon, S.; Shi, Q.; Jimenez, J. L.; Silva, P.
776 J.; Williams, P.; Lanni, T.; Drewnick, F.; Demerjian, K. L.; Kolb, C. E.; Worsnop D. R.
777 Chase studies of particulate emissions from in-use New York City vehicles. *Aerosol Sci.*
778 *Technol.* **2004**, *38*,555–573.

779 Canagaratna, M. R.; Jayne, J. T.; Jimenez, J. L.; Allan, J. D.; Alfarra, M. R.; Zang, Q., et al.
780 Chemical and microphysical characterization of ambient aerosols with the Aerodyne Aerosol
781 Mass Spectrometer. *Mass Spectrom. Rev.* **2007**, *26*,185–222.

782 Chirico, R.; DeCarlo, P. F.; Heringa, M. F.; Tritscher, T.; Richter, R.; Prevot, A. S. H.; Dommen,
783 J.; Weingartner, E.; Wehrle, G.; Gysel, M.; Laborde, M.; Baltensperger, U. Impact of
784 aftertreatment devices on primary emissions and secondary organic aerosol formation
785 potential from in-use diesel vehicles: results from smog chamber experiments. *Atmos. Chem.*
786 *Phys.* **2010**, *10*, 11545-11563.

787 Chirico, R.; Prevot, A. S. H.; DeCarlo, P. F.; Heringa, M. F.; Richter, R.; Weingartner, E.;
788 Baltensperger, U. Aerosol and trace gas vehicle emission factors measured in a tunnel using
789 an Aerosol Mass Spectrometer and other on-line instrumentation. *Atmos. Environ.* **2011**, *45*,
790 2182-2192, DOI: 10.1016/j.atmosenv.2011.01.069.

791 Chow, J. C.; Watson, J. G.; Lowenthal, D. H.; Chen, L. W. A.; Motallebl, N. $PM_{2.5}$ source
792 profiles for black and organic carbon emission inventories. *Atmos. Environ.* **2011**, *45*, 5407-
793 5414.

794 Cross, E S.; Sappok, A.; Fortner, E. C.; Hunter, J. F.; Jayne, J. T.; Brooks, W. A.; Onach, T. B.;
795 Wong, V. W.; Trimborn, A.; Worsnop, D. R.; Kroll, J. H. Real-time measurements of
796 engine-out trace elements: Application of a novel soot particle aerosol mass spectrometer for
797 emissions characterization. *J. Eng. Gas Turbines Power* **2012**, *134*, 072801.

798 Dallmann, T. R.; Harley, R. A.; Kirchstetter, T. W. Effects of diesel particle filter retrofits and
799 accelerated fleet turnover on drayage truck emissions at the Port of Oakland. *Environ. Sci.*
800 *Technol.* **2011**, *45*, 10773-10779, DOI:10.1021/es202609q.
801
802 Dallmann, T. R.; DeMartini, S. J.; Kirchstetter, T. W.; Herndon, S. C.; Onasch, T. B.; Wood, E.
803 C.; Harley, R. A. On-road measurement of gas and particle phase pollutant emission factors
804 for individual heavy-duty diesel trucks. *Environ. Sci. Technol.* **2012**, *46*, 8511-8518,
805 DOI:10.1021/es301936c.
806
807 Dallmann, T. R.; Kirchstetter, T. W.; DeMartini, S. J.; Harley, R. A. Quantifying on-road
808 emissions from gasoline-powered motor vehicles: Accounting for the presence of medium
809 and heavy-duty diesel trucks. *Environ. Sci. Technol.* **2013**, *47*, 13873-13881,
810 DOI:10.1021/es402875u.

811 DeCarlo, P. F.; Kimmel, J. R.; Trimborn, A.; Northway, M. J.; Jayne, J. T.; Aiken, A. C.; Gonin,
812 M.; Fuhrer, K.; Horvath, T.; Docherty, K. S.; Worsnop, D. R.; Jimenez, J. L. Field-
813 deployable, high-resolution, time-of-flight aerosol mass spectrometer, *Anal. Chem.* **2006**, *78*,
814 8281–8289.

815 Donahue, N. M.; Robinson, A. L.; Stanier, C. O.; Pandis, S. N. Coupled partitioning, dilution,
816 and chemical aging of semivolatile organics. *Environ. Sci. Technol.* **2006**, *40*, 2635-2643.

817 Evans, J. S.; Wolff, S. K.; Phonboon, K.; Levy, J. I.; Smith, K. R. Exposure Efficiency: An idea
818 whose time has come. *Chemosphere* **2002**, *49*, 1075-1091.

819 Freund, R.; Wetzel, R.; Shul, R.; Hayes, T. Cross-section measurements for electron-impact
820 ionization of atoms. *Phys. Rev. A* , **1990**,*41*, 3575–3595.

821 Fujita, E. M.; Zielinska, B.; Campbell, D. E.; Arnott, W. P.; Sagebiel, J. C.; Gabele, P. A.;
822 Crews, W.; Snow, R.; Clark, N. N.; Wayne, W. C.; Lawson, D. R. Variations in speciated
823 emissions from spark-ignition and compression-ignition motor vehicles in California's South
824 Coast Air Basin. *J. Air & Waste Manage. Assoc.* **2007**, *57*, 705-720.

825 Gerlofs-Nijland, M. E.; Dormans, J. A. M. A.; Bloemen, H. J. T.; Leseman, D. L. A. C.; Boere,
826 A. J. F.; Kelley, F. J.; Mudway, I. S.; Jimenez, A. A.; Donaldson, K.; Guastadisegni, C.;
827 Janssen, N. A. H.; Brunekreef, B.; Sandstrom, T.; van Bree, L.; Cassee, F. R. Toxicity of
828 coarse and fine particulate matter from sites with contrasting traffic profiles. *Inhal. Technol.*
829 **2007**, *19*, 1055-1069.

830 Grieshop, A. P.; Miracolo, M. A.; Donahue, N. M.; Robinson, A. L. Constraining the volatility
831 distribution and gas-particle partitioning of combustion aerosols using isothermal dilution
832 and thermodenuder methods. *Environ. Sci. Technol.* **2009**, *43*, 4750-4756.

833

834 Isaacman, G.; Wilson, K. R.; Chan, A. W. H.; Worton, D. R.; Kimmel, J. R.; Nah, T.; Hohaus,
835 T.; Gonin, M.; Kroll, J. H.; Worsnop, D. R.; Goldstein, A. H. Improved resolution of
836 hydrocarbon structures and constitutional isomers in complex mixtures using gas
837 chromatography-vacuum ultraviolet-mass spectrometry. *Anal. Chem.* **2012**, *84*, 2335-2342,
838 DOI: 10.1021/ac2030464.
839
840 Jayne, J. T.; Leard, D. C.; Zhang, X.; Davidovits, P.; Smith, K. A.; Kolb, C. E.; Worsnop, D. R.
841 Development of an aerosol mass spectrometer for size and composition analysis of
842 submicron particles. *Aerosol Sci. Technol.* **2000***, 33*, 49-70.

843 Jerrett, M.; Burnett, R. T.; Ma, R.; Pope, C. A., Krewski, D.; Newbold, B.; Thurston, J.; Shi, Y.;
844 Finkelstein, N.; Calle, E. E.; Thun, M. J. Spatial analysis of air pollution and mortality in Los
845 Angeles. *Epidemiology* **2005**, *16*, 727-736.

846 Jimenez, J. L.; Jayne, J. T.; Shi, Q.; Kolb, C. E.; Worsnop, D. R.; Yourshaw, I., Seinfeld, J. H.;
847 Flagan, R. C.; Zhang, X.; Smith, K. A.; Morris, J. W.; Davidovits, P. Ambient aerosol
848 sampling using the Aerodyne aerosol mass spectrometer. *J. Geophys. Res.* **2003***, 108*, 8425.

849 Kimmel, J. R.; Farmer, D. K.; Cubison, M. J.; Sueper, D.; Tanner, C.; Nemitz, E., Worsnop, D.
850 R.; Gonin, M.; Jimenez, J. L. Real-time aerosol mass spectrometry with millisecond
851 resolution. *Int. J. Mass Spectrom.* **2011***, 303,*15–26.

852 Kittelson, D. B.; Watts, W. F.; Johnson, J. P. On-road and laboratory evaluation of combustion
853 aerosols – Part 1: Summary of diesel engine results. *Aerosol Sci.* **2006**, *37*, 913-930.

854 Kleeman, M. J.; Riddle, S. G.; Robert, M. A.; Jakober, C. A. Lubricating oil and fuel
855 contributions to particulate matter emissions from light-duty gasoline and heavy-duty diesel
856 vehicles. *Environ. Sci. Technol.* **2008**, *42*, 235-242.

857 Kweon, C. B.; Okada, S.; Foster, D. E.; Bae, M. S.; Schauer, J. J. Effect of engine operating
858 conditions on particle-phase organic compounds in engine exhaust of a heavy-duty, direct-
859 injection (D.I.) diesel engine. *SAE Technical Paper Series* **2003**, *2003-01-0342*, 73-89.

860 Lapuerta, M.; Hernandez, J. J.; Ballesteros, R.; Duran, A. Composition and size of disel
861 particulate emissions from a commercial European engine tested with present and future
862 fuels. *P. I. Mech. Eng. D-J. Aut.* **2003**, *217*, 907-919.

863 Lipsky, E. M.; Robinson, A. L. Effects of dilution on fine particle mass and partitioning of
864 semivolatile organics in diesel exhaust and wood smoke. *Environ. Sci. Technol.* **2006**, *40*,
865 155-162.

866 Maricq, M. M. Chemical characterization of particulate emissions from diesel engines: A review.
867 *Aerosol Sci.* **2007**, *38*, 1079-1118.

Marshall, J. D.; Teoh, S.; Nazaroff, W. W. Intake fraction of nonreactive vehicle emissions in US urban areas. *Atmos. Environ.* **2005**, *39*, 1363-1371.

Massoli, P.; Fortner, E. C.; Canagaratna, M. R.; Williams, L. R.; Zhang, Z.; Sun, Y.; Schwab, J. J.; Trimborn, A.; Onasch, T. B.; Demerjian, K. L.; Kolb, C. E.; Worsnop, D. R.; Jayne, J. T. Pollution gradients and chemical characterization of particulate matter from vehicular traffic near major roadways: Results from the 2009 Queens College Air Quality Study in NYC. *Aerosol Sci. Technol.* **2012**, *46*, 1201-1218.

Matthew, B. M.; Middlebrook, A. M.; Onasch, T. B. Collection efficiencies in an Aerodyne aerosol mass spectrometer as a function of particle phase for laboratory generated aerosols. *Aerosol Sci. Technol.* **2008**, *42*, 884-898.

May, A. A.; Presto, A. A.; Hennigan, C. J.; Nguyen, N. T.; Gordon, T. D.; Robinson, A. L. Gas-particle partitioning of primary organic aerosol emissions: (1) gasoline vehicle exhaust. *Atmos. Environ*, **2013**, *77*, 128-139, DOI:10.1016/j.atmosenv.2013.04.060.

May, A. A.; Nguyen, N. T.; Presto, A. A.; Gordon, T. D.; Lipsky, E. M.; Karve, M.; Guitierrez, A.; Robertson, W. H.; Zhang, M.; Chang, O.; Chen, S.; Cicero-Fernandez, P.; Fuentes, M.; Huang, S.-M.; Ling, R.; Long, J.; Maddox, C.; Massetti, J.; McCauley, E.; Na, K.; Pang, Y.; Rieger, P.; Sax, T.; Truong, T.; Vo, T.; Chattopadhyay, S.; Maldonado, H.; Maricq, M. M.; Robinson, A. L. Primary gas and PM emissions from light and heavy duty vehicles. *Atmos. Environ.* **2014,** *88*, 247-260, DOI:10.1016/j.atmosenv.2014.01.046.

McLafferty, F. W.; Turecek, F. *Interpretation of Mass Spectra*; University Science Books: Mill Valley, CA, 1993.

Mohr, C.; Huffman, J. A.; Cubison, M. J.; Aiken, A. C.; Docherty, K. S.; Kimmel, J. R.; Ulbrich, I. M.; Hannigan, M.; Jimenez, J. L. Characterization of primary organic aerosol emissions from meat cooking, trash burning, and motor vehicles with high-resolution aerosol mass spectrometry and comparison with ambient and chamber observations. *Environ Sci. Technol.* **2009**, *43*, 2443-2449.

Mozejko, P.; Sanche, L. Cross sections for electron scattering from selected components of DNA and RNA. *Radiation Physics and Chemistry*, **2005**, *73*, 77–84. DOI:10.1016/j.radphyschem.2004.10.001.

Ning, Z.; Polidori, A.; Schauer, J. J.; Sioutas, C. Emission factors of PM species based on freeway measurements and comparison with tunnel and dynamometer studies. *Atmos. Environ.* **2008**, *42*, 3099-3114, DOI:10.1016/j.atmosenv.2007.12.039.

Onasch, T. B.; Trimborn, A.; Fortner, E. C.; Jayne, J. T.; Kok, G. L.; Williams, L. R.; Davidovits, P.; Worsnop, D. R. Soot particle aerosol mass spectrometer: Development, validation, and initial application. *Aerosol Sci. Technol.* **2012,** *46*, 804-817.

903 Pankow, J. F. An absorption model of gas/particle partitioning of organic compounds in the
904 atmosphere. *Atmos. Environ.* **1994**, *28*, 185-188.

905 Pope, C. A.; Dockery, D. W. Health effects of fine particulate air pollution: Lines that connect, *J.*
906 *Air Waste Manage. Assoc.* **2006**, *56*, 709-742.

907 Pottie, R. F. Cross sections for ionization by electrons. I. Absolute ionization cross sections of
908 Zn, Cd, and Te2. II. Comparison of theoretical with experimental values for atoms and
909 molecules. *J. Chem. Phys.* **1966**, *44*, 916.

910 Robinson, A. L.; Donahue, N. M.; Shrivastava, M. K.; Weitkamp, E. A.; Sage, A. M.; Grieshop,
911 A. P.; Lane, T. E.; Pierce, J. R.; Pandis, S. N. Rethinking organic aerosols: Semivolatile
912 emissions and photochemical aging. *Science*, **2007**, *315*, 1259-1262.

913 Robinson, A. L.; Grieshop, A. P.; Donahue, N. M.; Hunt, S. W. Updating the conceptual model
914 for fine particle mass emissions from combustion systems. *J. Air Waste Manage. Assoc.*
915 **2010**, *60*, 1204-1222.

916 Rogge, W. F.; Hildemann, L. M.; Mazurek, M. A.; Cass, G. R. Sources of fine aerosol. 2.
917 Noncatalyst and catalyst-equipped automobiles and heavy-duty diesel trucks. *Environ. Sci.*
918 *Technol.* **1993**, *27*, 636-651.

919 Roth, C. M.; Goss, K.; Schwarzenbach, R. P. Sorption of a diverse set of organic vapors to diesel
920 soot and road tunnel aerosols. *Environ. Sci. Technol.* **2005**, *39*, 6632-6637.

921 Sakurai, H.; Tobias, H. J.; Park, K.; Zarling, D.; Docherty, K. S.; Kittelson, D.; McMurry, P.;
922 Ziemann, P. J. On-Line measurements of diesel nanoparticle composition and volatility.
923 *Atmos. Environ.* **2003**, *37*, 1199–1210.

924 Salcedo, D.; Laskin, A.; Shutthanandan, V.; Jimenez, J. L. Feasibility of the detection of trace
925 elements in particulate matter using online high-resolution aerosol mass
926 spectrometry. *Aerosol Sci.Tech.* 2012, *46*, 1187-1200, DOI:10.1080/02786826.2012.701354.

927 Sappok, A.; Wong, V. Lubricant-derived ash properties and their effects on diesel particulate
928 filter pressure drop performance. *J. Eng. Gas Turbines Power* **2011**, *133(3)*, 032805.

929 Schauer, J. J.; Kleeman, M. J.; Cass, G. R.; Simoneit, B. R. T. Measurement of emissions from
930 air pollutant sources. 5. C_1-C_{32} organic compounds from gasoline-powered motor vehicles.
931 *Environ. Sci. Technol.* **2002**, *36*, 1169-1180, DOI:10.1021/es0108077.

932 Shah, S. D.; Cocker, D. R.; Miller, J. W.; Norbeck, J. M. Emission rates of particulate matter and
933 elemental and organic carbon from in-use diesel engines. *Environ. Sci. Technol.* **2004**, *38*,
934 2544-2550, DOI:10.1021/es0350583.

935 Shields, L. G.; Suess, D. T.; Prather, K. A. Determination of single particle mass spectral
936 signatures from heavy-duty diesel vehicle emissions for $PM_{2.5}$ source apportionment. *Atmos.*
937 *Environ.* **2007**, *41*, 3841-3852.

938 Slowik, J. G,; Stainken, K.; Davidovits, P.; Williams, L. R.; Jayne, J. T.; Kolb, C. E.; Worsnop,
939 D. R.; Rudich, Y.; DeCarlo, P. F.; Jimenez, J. L. Particle morphology and density
940 characterization by combined mobility and aerodynamic diameter measurements. Part 2:
941 Application to combustion-generated soot aerosols as a function of fuel equivalence ratio.
942 *Aero. Sci. Technol.* **2004**, *38*, 1206–1222, DOI:10.1080/027868290903916.

943 Sonntag, D. B.; Bailey, C. R.; Fulper, C. R.; Baldauf, R. W. Contribution of lubricating oil to
944 particulate matter emissions from light-duty gasoline vehicles in Kansas City. *Environ. Sci.*
945 *Technol.* **2012**, *46*, 4191-4199.

946 Spencer, M. T.; Shields, L. G.; Sodeman, D. A.; Toner, S. M.; Prather, K. A. Comparison of oil
947 and fuel particle chemical signatures with particle emissions from heavy and light duty
948 vehicles. *Atmos. Environ.* **2006**, *40*, 5224-5235.

949 Spikes, H. The history and mechanisms of ZDDP. *Tribology Letters* **2004**, *17*, 469-489.

950 Subramanian, R.; Khlystov, A. Y.; Cabada, J. C.; Robinson, A. L. Positive and negative artifacts
951 in particulate organic carbon measurements with denuded and undenuded sampler
952 configurations. *Aero. Sci. Technol.*, **2004**, *38*, 27-48.

953 Tawara, H; Kato, T. Total and partial ionization cross sections of atoms and ions by electron
954 impact. *Atomic Data and Nuclear Data Tables*, **1987**, *36*, 167–353.

955 Tobias, H. J.; Beving, D. E.; Ziemann, P. J.; Sakurai, H.; Zuk, M.; McMurry, P.; Zarling, D.;
956 Waytulonis, R.; Kittleson, D. B. Chemical analysis of diesel engine nanoparticles using a
957 nano-DMA/thermal desorption particle beam mass spectrometer. *Environ. Sci. Technol.*
958 **2001**, *35*, 2233-2243.

959 Tornehed, P.; Olofsson, U. Lubricant ash particles in diesel engine exhaust. Literature review
960 and modeling study. *P. I. Mech. Eng. D-J. Aut.* **2011**, *255*, 1055-1066.

961 Worton, D. R.; Isaacman, G.; Gentner, D. R.; Dallmann, T. R.; Chan, A. W. H.; Kirchstetter, T.
962 W.; Wilson, K. R.; Harley, R. A.; Goldstein, A. H. Unburned lubricating oil dominates
963 primary organic particulate emissions from motor vehicles. *Environ. Sci. Technol.* **2014**, *48*,
964 3698-3706, DOI:10.1021/es405375j.

965

966

967

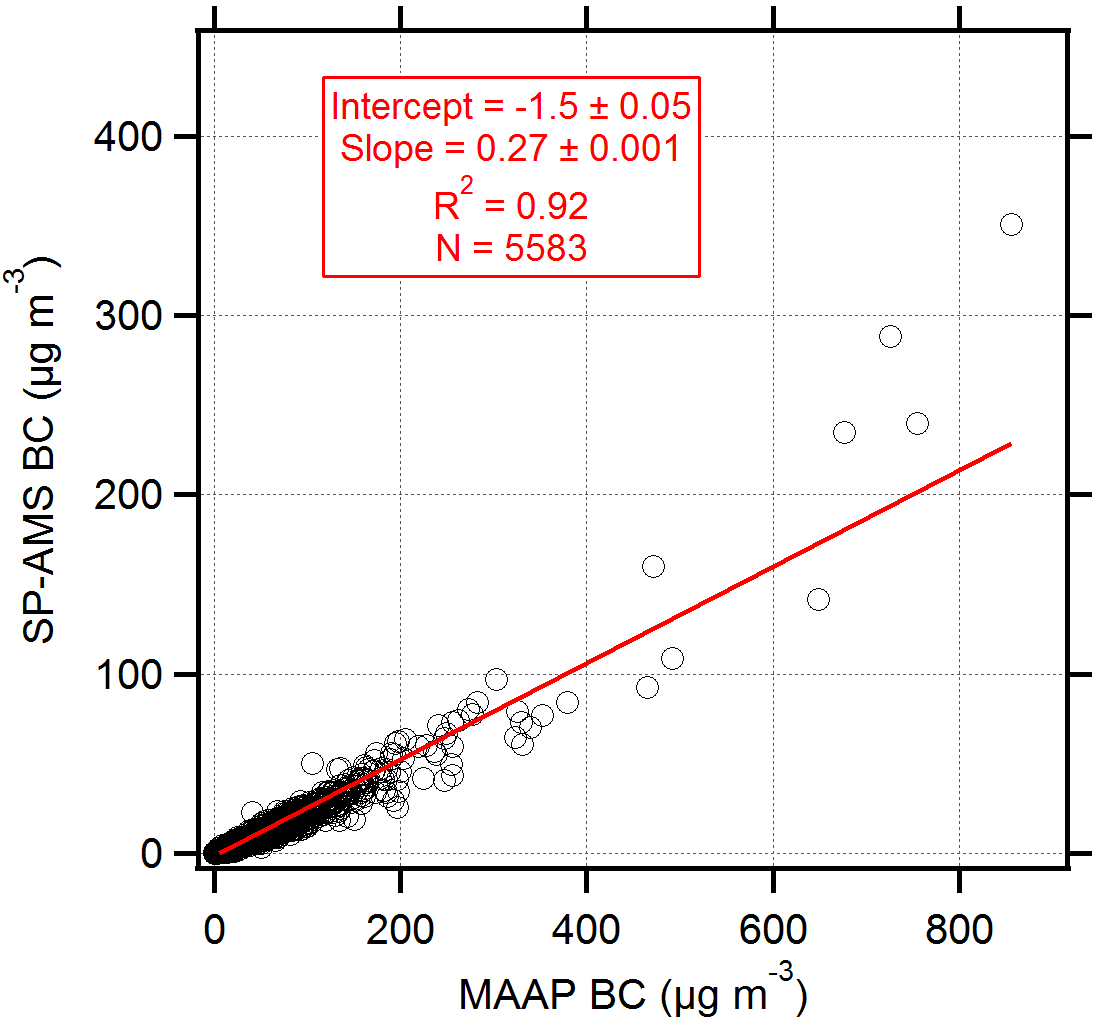

968

969 **Figure 1.** Comparison of 10 s average BC concentrations measured by SP-AMS and MAAP

970 instruments. The slope of the linear fit describes the SP-AMS collection efficiency for BC as

971 0.27.

972

973

974

975

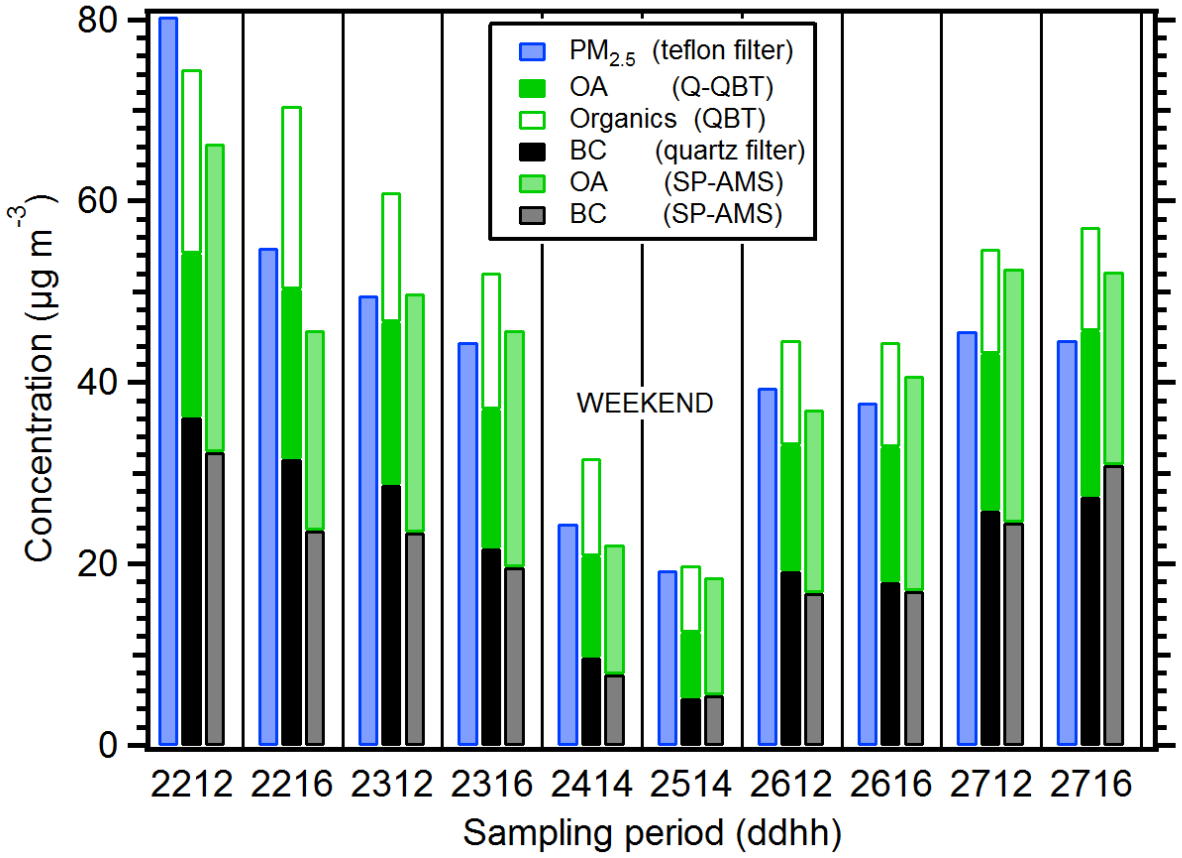

976

977 **Figure 2.** Comparison of average $PM_{2.5}$ concentrations and composition measured during each
978 2-hr sampling period. Three measures of $PM_{2.5}$ mass are shown for each period, derived (reading
979 left to right) from analysis of Teflon filters, quartz filters, and SP-AMS data. Sampling periods
980 are identified using codes of the form ddhh, where dd indicates the day during July 2010, and hh
981 is the starting hour of sampling. July 24 and 25 in the middle of the figure were weekend days
982 with lower diesel truck traffic volumes. Q-QBT OA concentrations correspond to quartz filter-
983 derived OA measurements adjusted to account for organics measured on separate quartz-behind-
984 Teflon (QBT) filter samples collected in parallel. QBT organic concentrations are also shown
985 here as unshaded green bars.

986

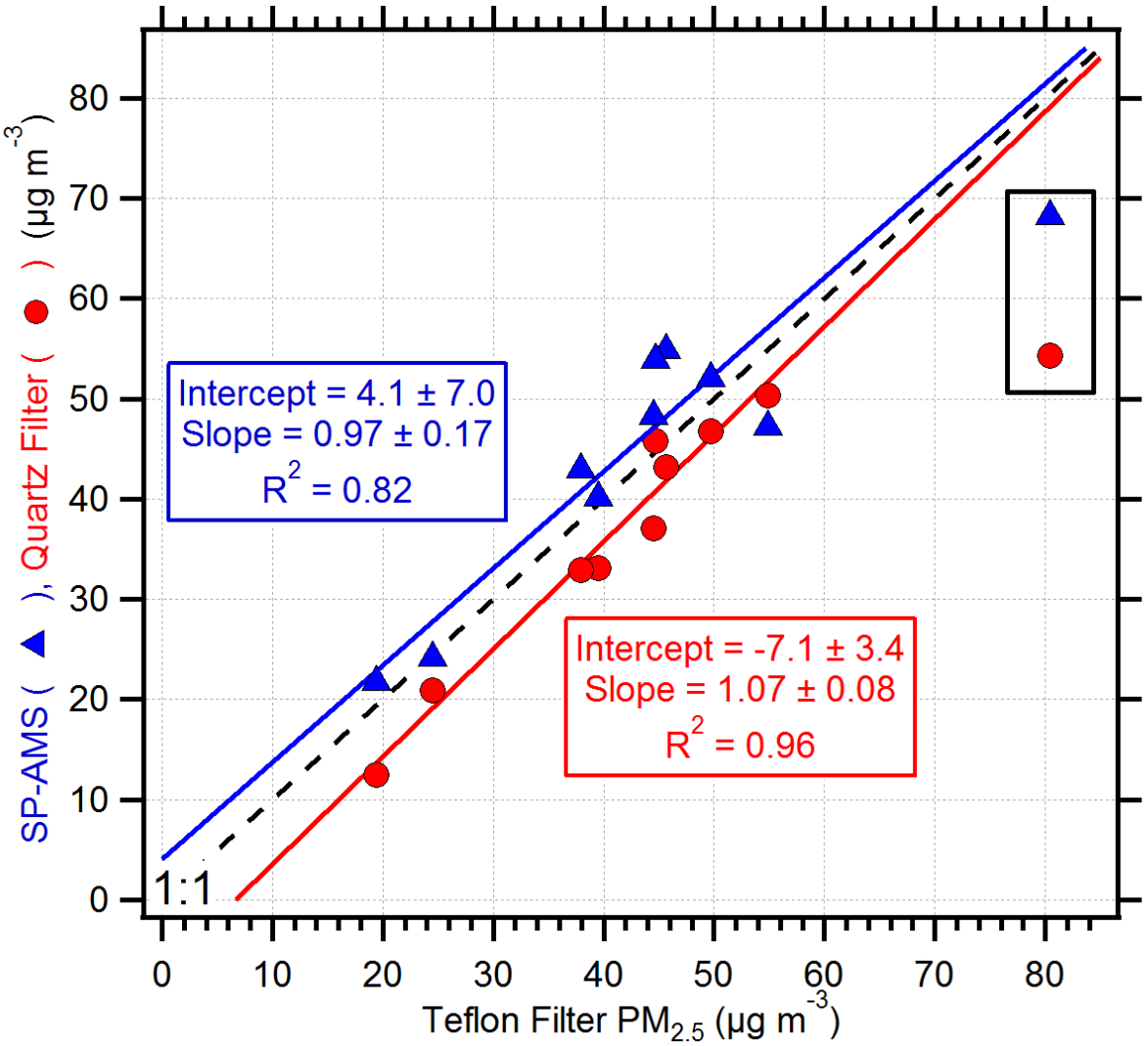

987

988 **Figure 3**. Comparison of gravimetrically determined $PM_{2.5}$ mass concentrations and (blue
989 triangles) SP-AMS total mass including carbonaceous species (OA, BC) as well as inorganic
990 ions (sulfate, nitrate, ammonium, chloride), and (red circles) carbonaceous species (OA, BC)
991 determined from thermal-optical analysis of quartz filter samples. Boxed points at the right of the
992 figure were excluded from the regression analysis due to an anomalous street sweeping event
993 that occurred during the IOP2212 sampling period.

994

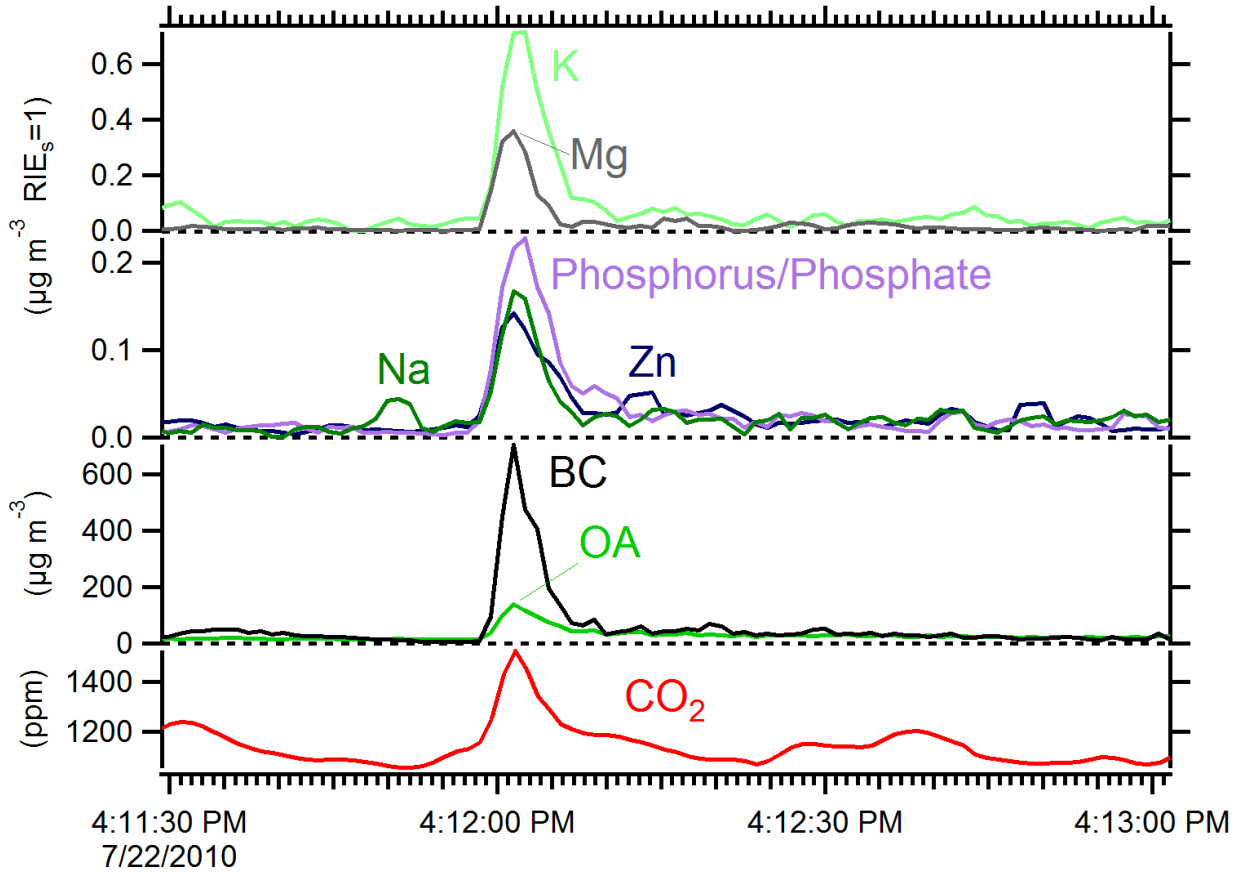

995

996 **Figure 4.** Species concentrations measured during individual diesel truck plume event. Clear

997 peaks are visible for trace elements, indicating presence in truck exhaust plume.

998

999

1000

1001

1002

1003

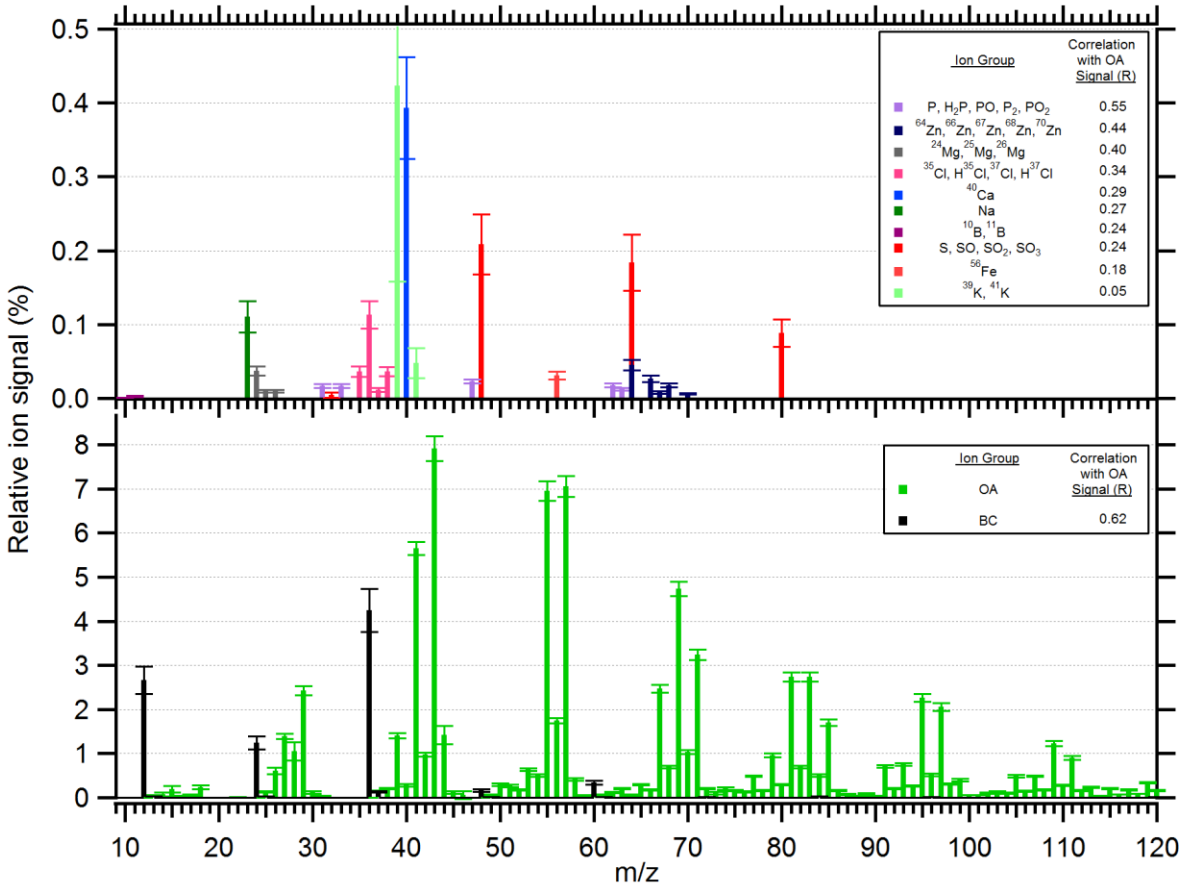

1004

1005 **Figure 5.** Average relative ion signal for 145 diesel truck exhaust plumes. Error bars show 95%

1006 confidence interval. Legend includes correlation of signal from each ion group with the total OA

1007 signal.

1008

1009

1010

1011

1012

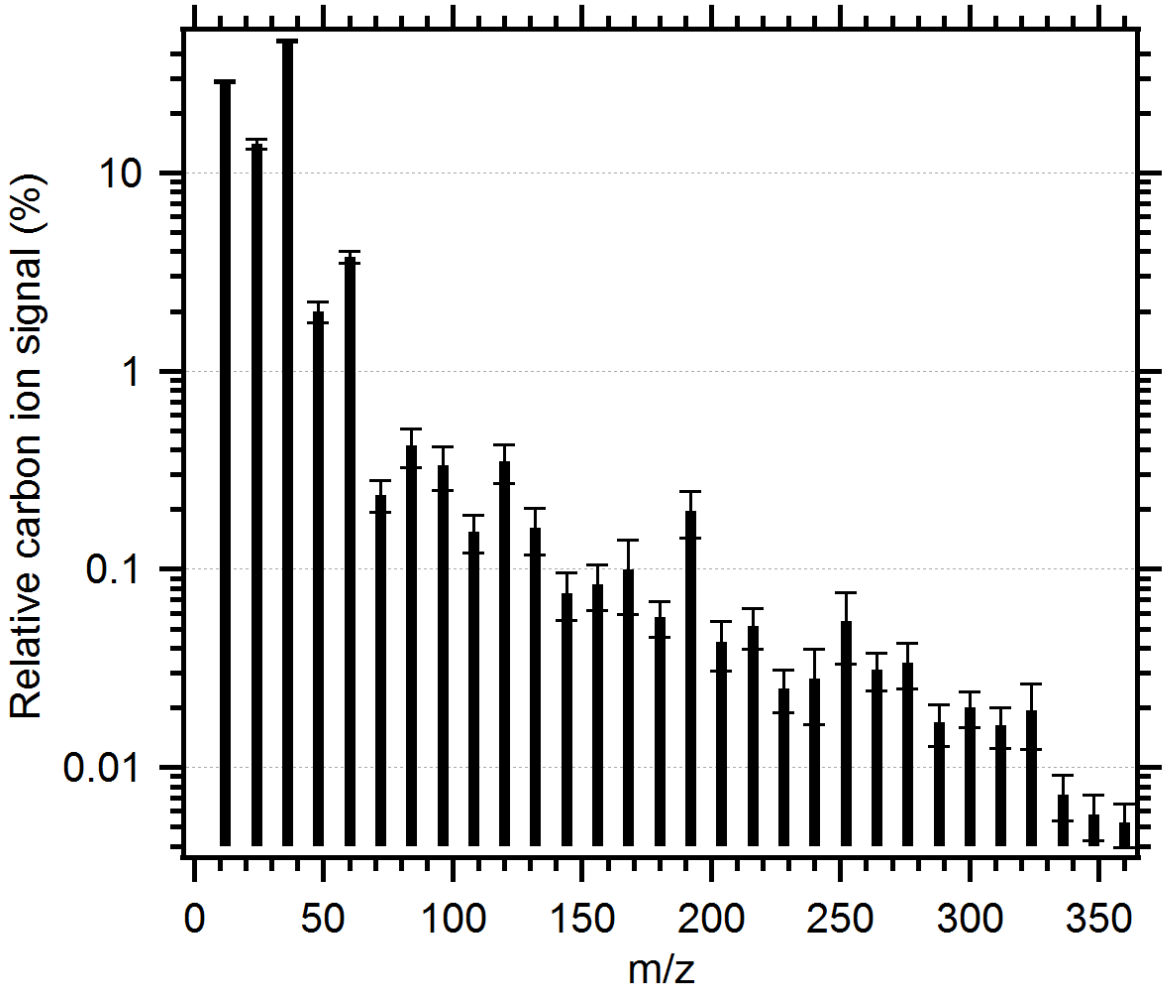

Figure 6. Average BC mass spectra for 145 diesel truck plumes. Ion signals for each carbon ion (C_x^+) are normalized to total carbon ion signal. Note ^{13}C isotopes are excluded here for sake of visual clarity.

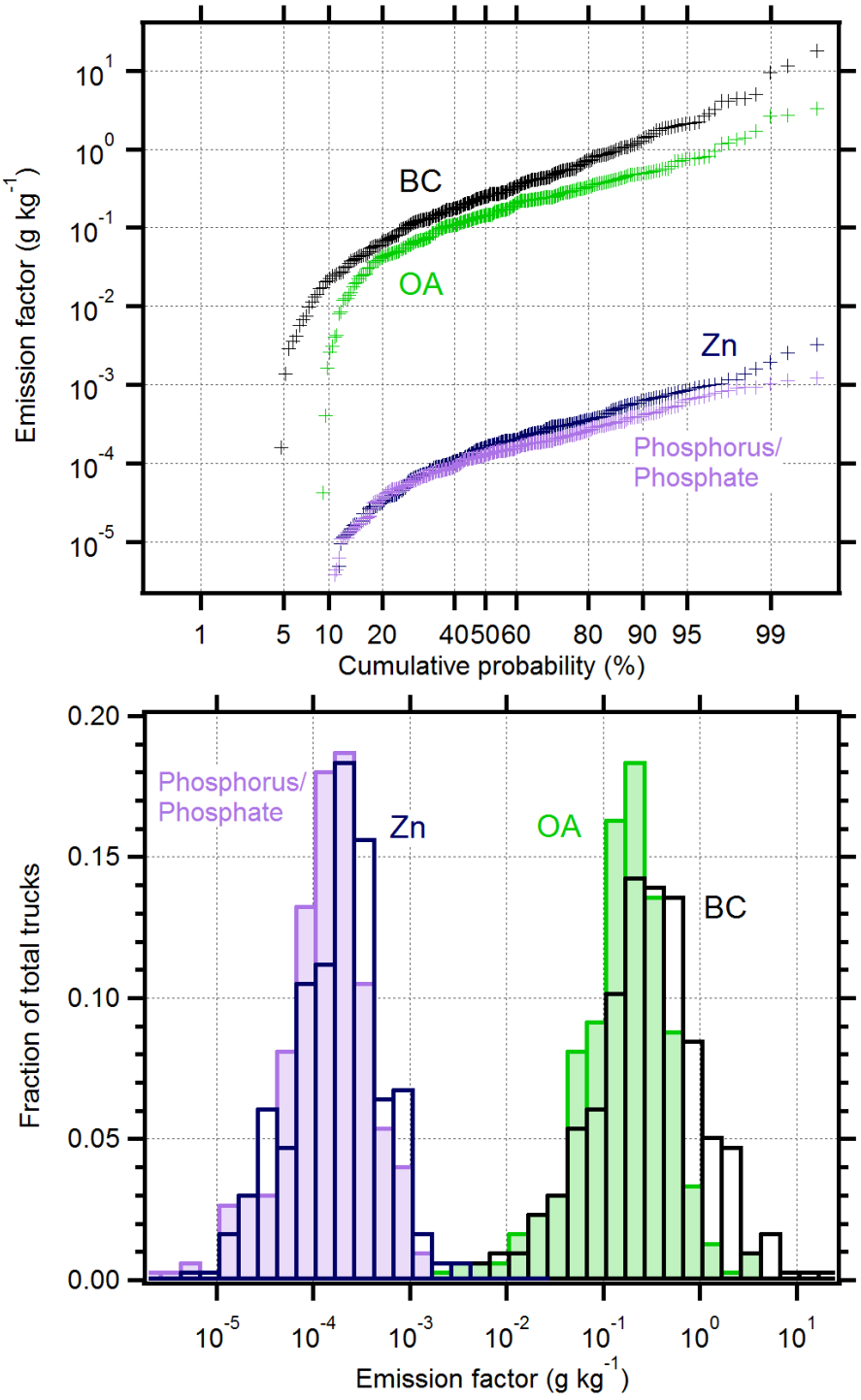

1021

1022 **Figure 7.** Emission factor log-probability plots (top) and distributions (bottom) for OA, BC,

1023 zinc, and phosphorus/phosphate.

1024

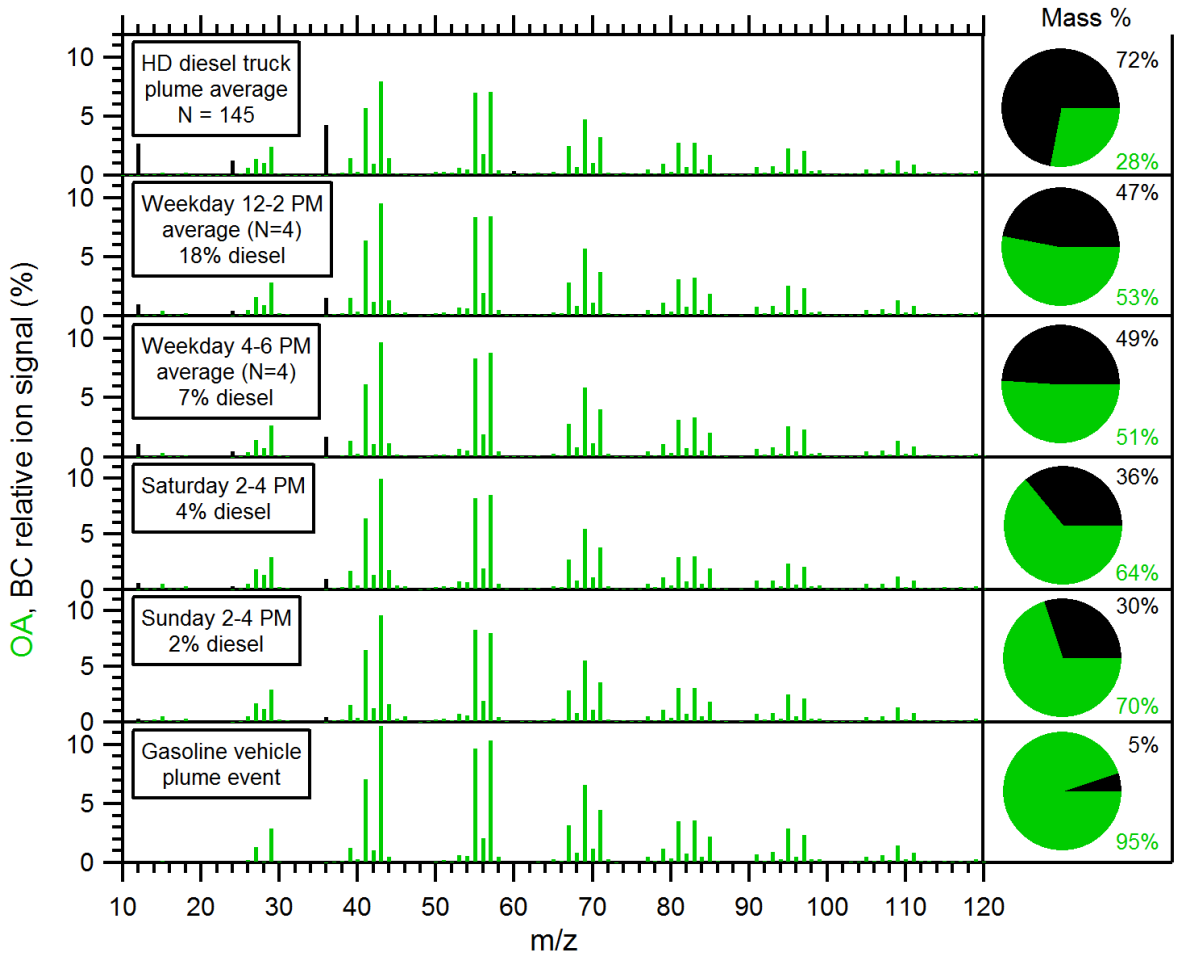

1025

1026 **Figure 8.** OA (green) and BC (black) mass spectra for high (top panel) to low (bottom panel)

1027 levels of diesel truck influence. Pie charts show relative contributions of OA and BC to total

1028 carbonaceous mass.

1029

1030

1031

1032

1033

1034

1035

1036

1037 **Table 1**. Fleet-average emission factors for HD diesel trucks (N=293).

Species	Emission factor ± 95% confidence interval	Emission factor units	Emission factor ratio to OA emission factor (ppm)	Lubricating oil elemental weight fraction (ppm)[a]
BC	0.62 ± 0.17	g kg^{-1}		
OA	0.24 ± 0.04	g kg^{-1}		
Zinc	0.26 ± 0.04	mg kg^{-1}	1100 ± 250	1226
Phosphorus/ phosphate	0.18 ± 0.02	mg kg^{-1}	760 ± 160	985

1038 [a]Lubricating oil elemental composition reported for a SAE 15W-40 CJ-4 diesel engine oil
1039 (Sappok and Wong, 2011).

1040

1041 **Table 2.** Molar element ratios and OA/OC mass ratios for on-road motor vehicle emissions.

Sampling period	O/C	H/C	OA/OC
HD Diesel truck plume average (N=145)	0.06 ± 0.02	1.90 ± 0.05	1.24 ± 0.03
Weekday 12-2 PM average (N=4)	0.07 ± 0.04	1.89 ± 0.05	1.25 ± 0.05
Weekday 4-6 PM average (N=4)	0.06 ± 0.03	1.91 ± 0.04	1.24 ± 0.03
Saturday 2-4 PM	0.09 ± 0.04	1.87 ± 0.07	1.28 ± 0.06
Sunday 2-4 PM	0.10 ± 0.05	1.86 ± 0.08	1.30 ± 0.07
High-emission gasoline vehicle	0.020 ± 0.003	1.99 ± 0.01	1.192 ± 0.004

1042